European Commission

JRC TECHNICAL REPORTS

Cold atom interferometry for Earth observation

Perspectives for satellite-based quantum gravimetry

Travagnin, M.

2020

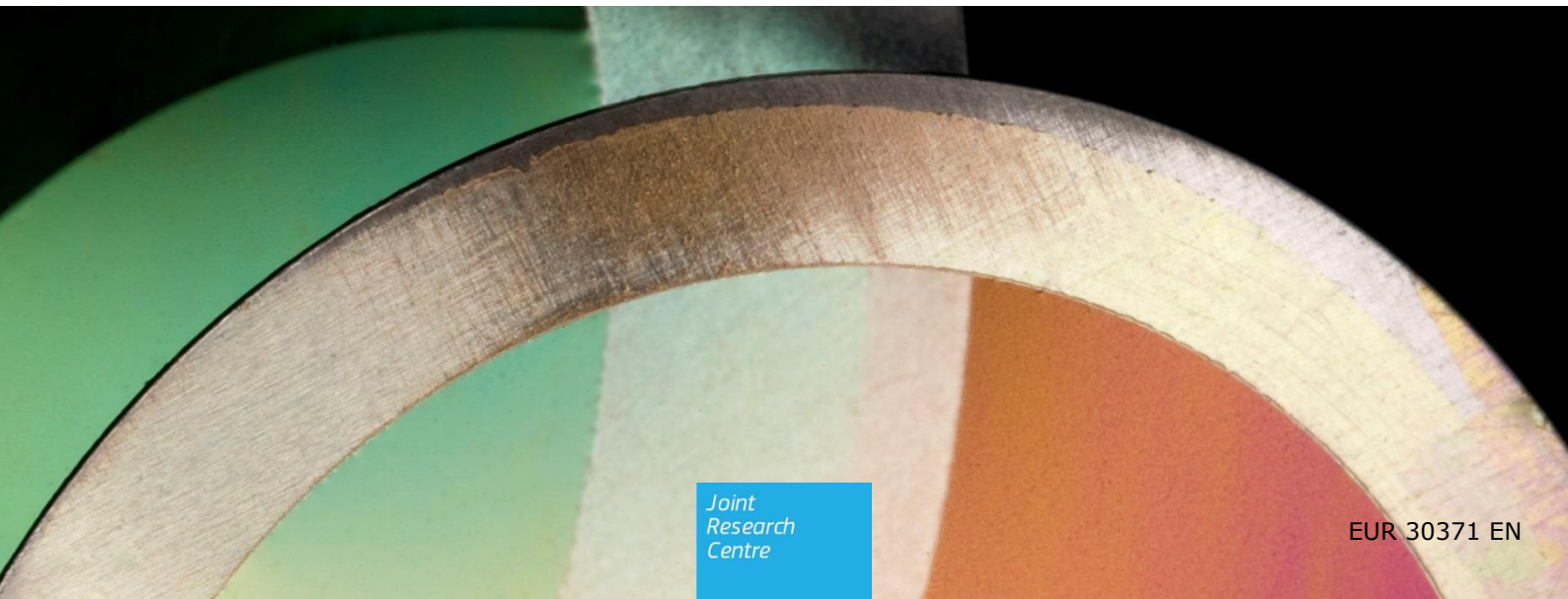

EUR 30371 EN

Contact information
Name: Martino Travagnin
Email: Martino.Travagnin@ec.europa.eu

EU Science Hub
https://ec.europa.eu/jrc

JRC121833

EUR 30371 EN

PDF ISBN 978-92-76-21686-5 ISSN 1831-9424 doi:10.2760/225071

Luxembourg: Publications Office of the European Union, 2020

How to cite this report:

M. Travagnin, *Cold atom interferometry for Earth observation: Perspectives for satellite-based quantum gravimetry,* 2020, EUR 30371 EN, Publications Office of the European Union, Luxembourg, 2020, ISBN 978-92-76-21686-5, doi:10.2760/225071, JRC121833

Contents

Acknowledgements

This work has been done in the framework of the SynQArc administrative arrangement between DG JRC and DG DEFIS. I am glad to acknowledge continuous help from my JRC colleague Adam Lewis, and useful conversations with several DG DEFIS colleagues.

Abstract

This report provides an assessment on cold atom interferometry (CAI) gravity sensing for Earth Observation (EO), and is intended as an instrument to facilitate the interactions between the different communities involved in the definition of a related satellite mission. Indeed, the definition of the objectives of future gravity missions and of the technologies needed for their implementation is the result of complex negotiations and compromises: geodesy and geophysics researchers detail the scientific requirements dictated by their investigation areas (e.g. solid Earth dynamics, ocean mass and heat transport, ice sheets and glaciers evolution), policymakers express their concerns and their priorities (e.g. natural hazards risk assessment, ground water monitoring, floods and droughts forecast), engineers and technology experts devise and implement the most suitable techniques to actually build the satellite and its gravity sensing payload.

As we will show in this report, the scientific consensus is that the scientific objectives of a next generation gravity mission (NGGM) to be deployed within a ~10 year timeframe can be achieved by upgrading established technologies already used in gravity-measuring satellites. Transformative technologies such as CAI-based gravity sensors leveraging Bose Einstein Condensates (BEC) of ultra-cold atoms may come to play a role in the longer term, provided that several technology challenges are overcome; in addition, further interdisciplinary work and the simulation of detailed mission scenarios are needed to fully establish their actual usefulness with regards to the attainment of future gravity missions scientific objectives.

The scientific community seems to agree on the opportunity of an intermediate stepping stone, which could take the form of a scientific mission with a dedicated satellite, in order to test and prove the in-space feasibility and the actual usefulness of CAI-based gravity sensors.

1 Introduction

This technical report addresses the possible use of cold atom interferometry (CAI) for Earth observation, and more specifically for satellite-based gravimetry. It is the third one in a series which is intended to provide a guide for policymaking in a rapidly evolving area of quantum technologies, cold atom interferometry sensing, which holds the promises for applications in fields where the EU has well established programmes, or plans to upscale its action[1,2]. Although an effort has been made to make the report self-contained, the reader interested in a basic understanding of the phenomena leveraged for the applications here analysed is addressed to the physics and technologies background described in the first one in the series, JRC121223.

We emphasize that the present work does not cover the use of space-based interferometry with cold or ultra-cold atoms for scientific missions aimed at fundamental physics experiments: in the last ~20 years an extremely rich scientific literature flourished to explore this theme and several proposals have been advanced by the scientific community, which are now at various implementation stages; to cap this all, space-based technology tests have recently been performed. Indeed, earthbound CAI is already a well-established tool for scientific investigations, and since its deployment in the microgravity environment enabled by deployment in space would allow a notable increase of sensitivity, it is all too natural for scientist interested in testing fundamental physics theories to be keen on it. Conversely, the use of space-based CAI for Earth observations aimed at eminently practical applications has a much less rich and articulated history, having started only recently to attract the interest of researchers and policymakers. In part for this, but in part maybe also for deeply-rooted technical reasons, its actual in-field advantages with respect to existing and evolving consolidated technologies have not yet been firmly established.

Let us recall that the definition of future Earth observation gravity missions implies a number of quite complex interactions: indeed, on one side there are the different scientific communities which study the various phenomena that can be monitored thanks to space-based gravity measurements, and on the other hand we have the policymakers who are called to define on a much wider scene the environmental and societal priorities that the scientific work has to help achieving. In more concrete terms, the scientific objectives of future gravity missions are to be determined by geophysics and geodesy researchers which measure mass distribution and monitor mass transport processes which take place on solid Earth, oceans, cryosphere, atmosphere and hydrosphere. In the meanwhile, policymakers express their concerns on concrete problems such as floods and droughts forecasting, coastal vulnerability, climate impact on ice sheets, water management, ground water monitoring, natural hazards risk assessment, etc.: managing these issues require the backing of reliable and long-term data, which are expected in great part to come from space-based gravity missions. Interfacing these political priorities with the scientific ones allows defining the objectives of future space gravimetry missions, whose actual implementation is a task left to a wide array of technology experts, covering the different disciplines needed to build a satellite-based gravity sensor. The main aim of this report is to establish an objective and unbiased background to help this policy-science-technology trilogue, highlighting the potentials of satellite-based CAI gravity sensors without hiding their expected limitations and the challenges to be overcome for their actual adoption.

The report starts by presenting in Section 2 a brief recap of the most recent satellite-based gravimetry missions, which constitute the backdrop point against which the

[1] "Cold atom interferometry sensors: physics and technologies. A scientific background for EU policymaking", M. Travagnin, JRC121223, 2020; https://ec.europa.eu/jrc/en/publication/cold-atom-interferometry-sensors-physics-and-technologies

[2] "Cold atom interferometry for inertial navigation sensors. Technology assessment: space and defence applications", M. Travagnin, JRC121225, 2020; (Sensitive, limited distribution)

performances of future gravity missions have to be defined. In Section3 it summarizes the work and the activities which in the last decades have taken place to define the scientific objectives of so-called next generation gravity missions (NGGM), showing how the various scientific communities interested in monitoring different phenomena have often express differing and sometimes contrasting desires, which have then also to be weighted in terms of their impact for the priorities expressed by policymakers. A delicately-balanced synthesis therefore defines the objectives of future gravity missions, and the panorama is still not clearly defined, especially when the time horizon extends beyond the next ~10 years. In Section 4 we show how the scientific consensus is that a smooth and continuous evolution of existing technologies already deployed in space could meet the technological requirements needed to fulfil the scientific aims of NGGM in the next ~10 years, while CAI-based gravimetry could play a role in the longer term. In Section 5 we review the main proposals which have been advanced on the use of CAI sensors for future gravity missions, and we assess the state of the art. A brief glossary to help the reader with the most cryptic technical expression is provided in Section 6, and the work conclusions are summarized in Section 7.

2 State of the field

In this paragraph we provide the essential backdrop against which a gravimetry mission must be assessed, by giving some basic information about the past dedicated gravity missions CHAMP, GRACE and GOCE.

CHAMP was a DLR mission, operating in 2000-2010. It consisted in a single satellite, with onboard accelerometers and high-low satellite-satellite tracking. In simpler terms, this means that the position of the CHAMP satellite was determined by using a positioning system based on the GPS constellation. The initial orbital height was 450km, which diminished as the mission progressed. The gravity field was obtained by comparing the expected satellite position with the actual one, and taking into account the non-gravitational contribution of the acceleration, as measured by the on-board accelerometers and as deduced by appropriate physical models. The Earth dynamical gravity field was retrieved with a ~700km spatial resolution, a seasonal (some months) temporal resolution, and a geoid accuracy of some centimetres. We recall that the geoid is a surface of equal gravitational potential which, over the oceans, corresponds to mean sea-level.

The GRACE mission, by NASA and DLR, took place in 2002-2017, and a very similar GRACE-FO (follow-on) mission, started in 2018, is now operational. GRACE employs a pair of satellites, orbiting at a height of ~500 km at a distance of ~220 km. It also makes use of onboard accelerometers and satellite tracking. The gravity field is deduced from the distance between the satellites, which is measured via a microwave interferometric link (with a precision of ~10μm). Laser interferometry (precision ~1μm) is deployed as technological demonstrator in the GRACE-FO satellites. The geoid is obtained with a spatial resolution of 300-500km and a sub seasonal (monthly) temporal resolution, with a ~1cm accuracy.

GOCE was an ESA mission, consisting in a single satellite orbiting at low altitude (~260km) from 2009 to 2013. The main satellite instrument was a gravity gradiometer, which measured the variations of all the acceleration components along three different directions. GOCE also used satellite-to-satellite tracking, with reference to GPS satellites, to measure non-gravitational accelerations. From the gravity gradiometer signal, and a precise attitude of positioning of the satellite, the stationary gravity field was obtained with a ~100km resolution and a geoid accuracy better than 1cm.

We have therefore seen that one of the main aims of satellite-based gravity missions is the precise determination of the geoid, which is the smooth but irregular surface determined by the uneven distribution of mass below and on the surface of Earth, see Fig. 1.

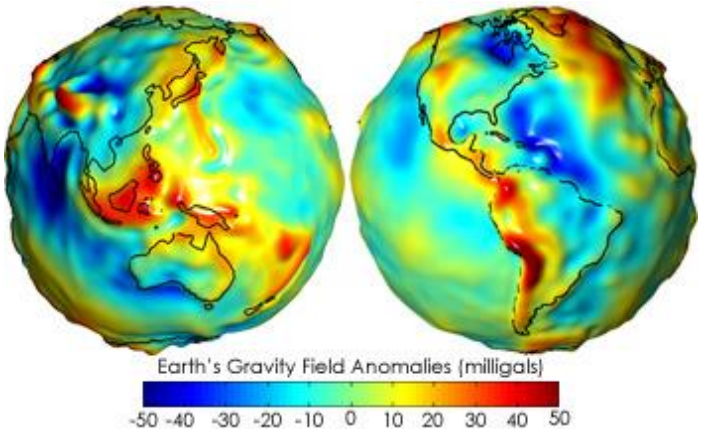

Fig. 1: Map of geoid undulations determined by gravity field anomalies, measured in milliGalileo (mGal). We recall that 1mGal = 10^{-3}Gal = 10^{-5}m/s^2 ≈ 10^{-6}g, where g ≈ 9.81m/s^2 is the gravity acceleration on the Earth surface. A gravity anomaly of 1 milliGal (=1μg) roughly corresponds to a geoid height of 1cm. The last ~20 years of satellite observations allowed determining the geoid with an accuracy of ~1cm (~1mGal, ~10^{-6}g). Figure source: https://earthobservatory.nasa.gov/features/GRACE/page3.php.

By taking into account only rotation and self-gravitation, and under several simplifying assumptions, the planet gravity field is described by an ellipsoid of revolution. The gravity anomaly is defined as the difference in any given point on the planet's surface between the observed gravity (i.e. the free-fall acceleration), and the corresponding value predicted by the reference ellipsoid. Gravity anomalies have the most disparate causes, which are the objects of disciplines such as geodesy and geophysics.

In Fig. 2 we give a pictorial representation of the phenomena which can be monitored with the time and space resolution achieved by the CHAMP, GRACE, and GOCE missions.

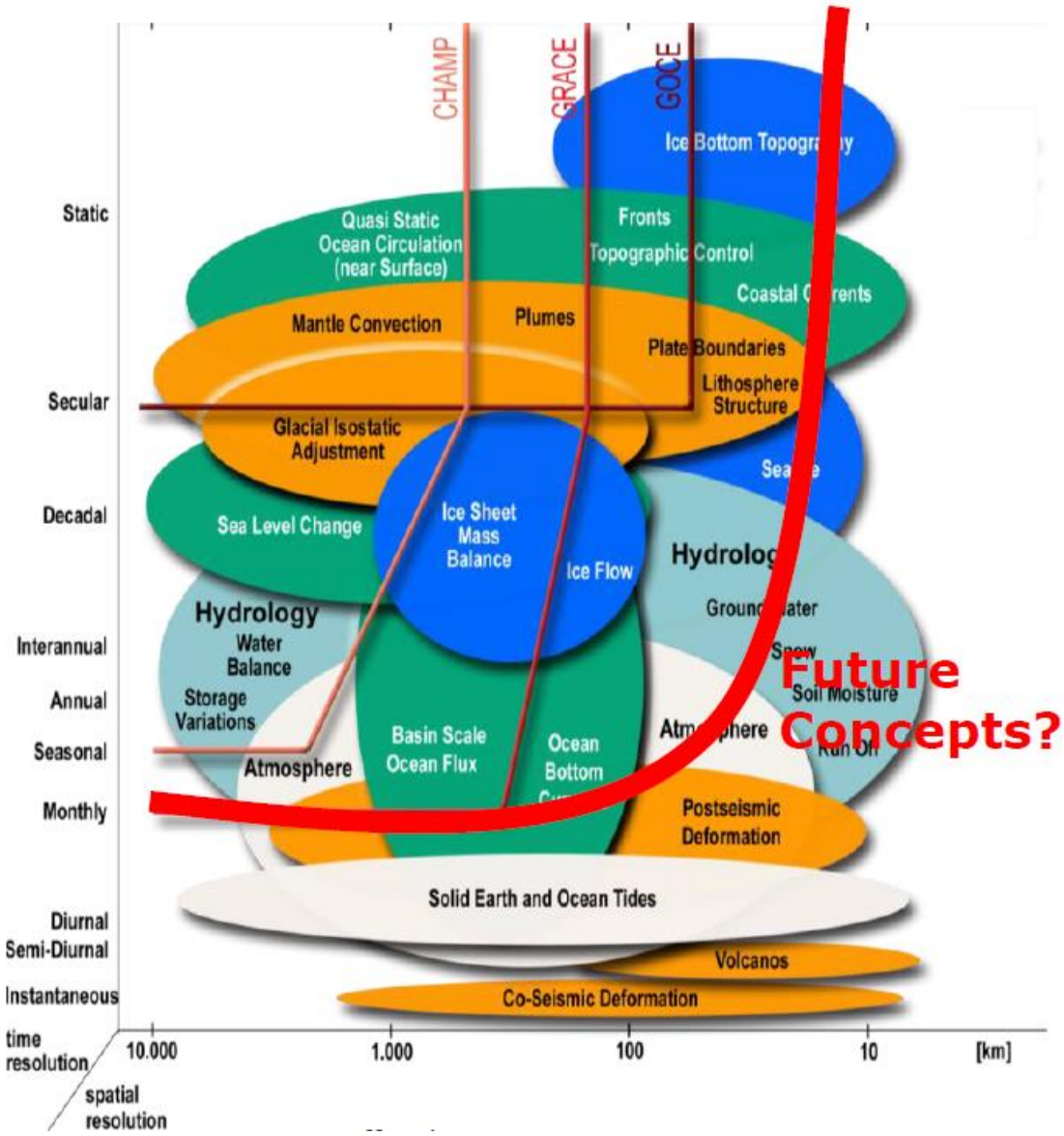

Fig. 2: Geophysical phenomena monitored by satellite gravity missions. Time and space resolution achieved by the CHAMP, GRACE and GOCE missions are shown. The thick red line delimits the area thought to become accessible in next generation gravity missions based on existing technological building blocks[3]

[3] "The ESA Earth Observation Programmes Activities for the Preparation of the Next Generation Gravity Mission", L. Massotti et at., Guidance, Navigation, and Control Conference, 2013 https://www.researchgate.net/publication/268469839_The_ESA_Earth_Observation_Programmes_Activities_for_the_Preparation_of_the_Next_Generation_Gravity_Mission

In mathematical terms, spherical harmonics (SH) are usually used to approximate the shape of the geoid, by expanding the corresponding gravity potential as the sum of a series:

$$V(r,\vartheta,\lambda) = \frac{GM}{R}\sum_{n=0}^{N}\left(\frac{R}{r}\right)^{n+1}\sum_{m=0}^{n}\left[\bar{C}_{nm}\cos m\lambda + \bar{S}_{nm}\sin m\lambda\right]\bar{P}_{nm}(\cos\vartheta)$$

Here GM is the gravitational constant of the Earth, R is the radius of Earth, (r,ϑ,λ) are spherical coordinates of a point on the Earth surface (radius, co-latitude, longitude), n,m denote SH degree and order, N denotes the maximum degree of the model expansion (in theory ∞), $\bar{P}_{nm}(\cos\vartheta)$ are the fully normalized associated Legendre functions, and $\bar{C}_{nm}$, $\bar{S}_{nm}$ are the normalized SH coefficients, which are the unknowns of the gravity field solution. The higher the degree of the expansion, the higher the spatial resolution of the gravity potential, as can be deduced from Fig. 3.

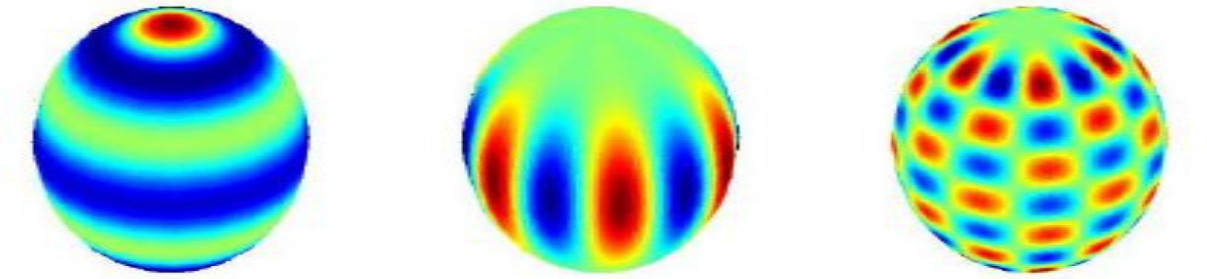

Fig. 3: Examples of spherical harmonic functions, which constitute the basis for the series expansion of the gravity potential. Higher spherical harmonic degrees correspond to better spatial resolution[4].

In Fig. 4 we show the cumulative geoid error height of the three missions, as a function of the spherical harmonic degree. It can be seen that GRACE improves the performance of CHAMP for all the SH degrees, meaning for all spatial resolutions. GOCE ensures lower error than GRACE at SH degrees higher than ~60, meaning that it is able to reach finer spatial detail, at the price of not being able to provide their temporal variation. Grace can provide extremely accurate description (i.e. with low geoid errors) of global scale phenomena, which occur on large spatial scale, as can be deduced from its low error level at low SH degrees. We recall (see also Fig. 2) that GRACE provides also a monthly retrieval of the gravity field, as compared by the CHAMP seasonal retrieval. GOCE guaranteed an even higher spatial resolution, but only for quasi-stationary gravity field (secular time resolution). GRACE-FO will constitute a substantial improvement both with respect to GOCE (especially at lower degrees) and with respect to GRACE (especially at higher degrees). To make more intuitive the interpretation of the figure, we report in the following Table 1 the correspondence between some values of spherical degree and the spatial resolution.

Spherical degree	20	30	80	100	200	300
Spatial resolution (km)	1000	650	250	200	100	70

Table 1: Half-wavelength spatial resolution corresponding to increasing spherical degrees

[4] "Lectures on gravity field basics and GRACE", R. Forsberg, ESA Cryosphere Training Course, 2016 http://seom.esa.int/cryotraining2016/files/CTC16/Day4/3_Forsberg_grace_sep2016%202.pdf

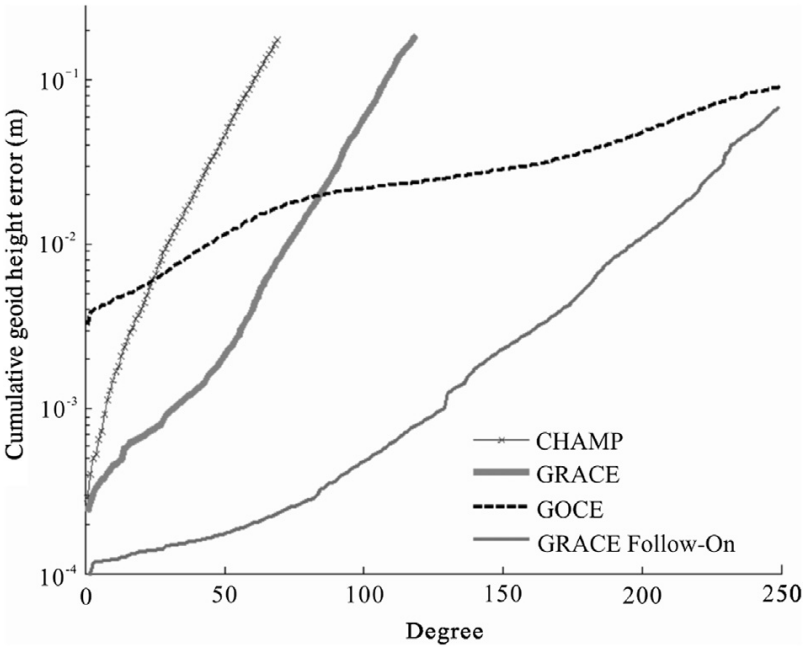

Fig. 4: Cumulative geoid error height of the CHAMP, GRACE, GOCE, and GRACE-FO missions as a function of the spherical harmonic degree. As a general rule the error increases with the degree, meaning that the magnitude of small-scale features will be affected by a higher uncertainty[5].

As we have already seen in a previous report, and as we will see later in greater detail, atomic interferometry can be leveraged to build absolute accelerometers based on the inertial properties of atoms, with distinctive advantages in terms of sensitivity and long term stability. Since accelerometers lay at the core of a gravity mission, there is a clear potential for the use of CAI accelerometers in future gravity missions. The main point to be addressed is: to which extent exploiting novel technologies based on atomic interferometry can actually guarantee a lower geoid error, for which range of spherical harmonic degrees and with which temporal resolution? As we will see, to answer these questions a narrow assessment of the technology itself does not suffice, and the view must be broadened to include full mission simulations.

[5] "Progress in satellite gravity recovery from implemented CHAMP, GRACE and GOCE and future GRACE-FO missions", Zheng Wei et al., Geodesy and Geodynamics, Vol. 6, No. 4, 2015
https://www.sciencedirect.com/science/article/pii/S1674984715000506

3 Science and policy targets for future gravity missions

Establishing the priorities of a satellite-based gravity mission is both a scientific and a policy issue. Broadly speaking, such missions are intended to measure mass distribution and monitor mass transport processes which take place on different time scales on the solid Earth, oceans, cryosphere, atmosphere and hydrosphere. Several scientific challenges can be addressed, each on them linked to political priorities. A possible graphic representation is provided by the double-shell graph shown in Fig. 5: to give an example, the political priority of addressing costal vulnerability will require the data provided by several scientific topics, such as monitoring the sea level rise, separating natural and anthropogenic processes, investigating heat transport in the ocean mass, and many others. Historically, a methodology emerged by which the different scientific communities involved put forward their target proposals, which are then discussed in view of the possible technological implementation. A widely shared understanding is the need for data consistency and long-term continuity, in addition with improved accuracy. The relative importance of higher space resolution and higher temporal resolution depends on the particular science objective being pursued.

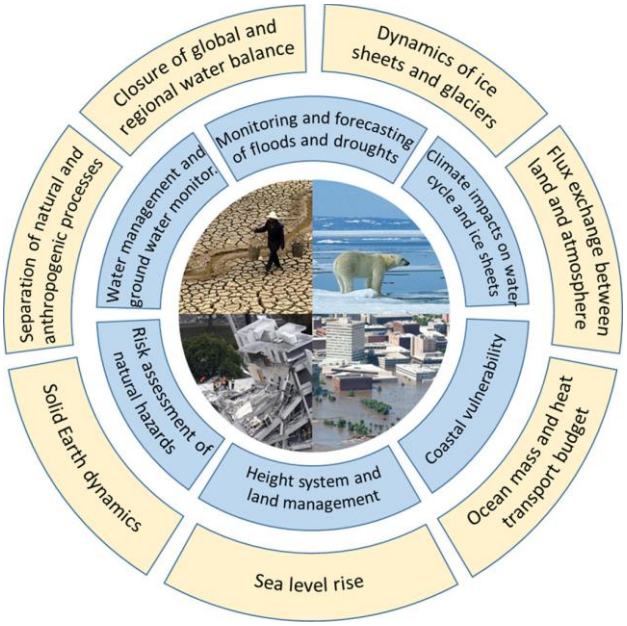

Fig. 5: Schematic representation of some of the scientific (outer shell) and policy (inner shell) priorities which may play a role in the definition of a gravity mission. The figure is taken from the IUGG 2015 study, see later for more details.

A first example of this approach is a 2013 ESA preparatory study, which involved ~70 representatives from earth-related disciplines (geophysics and geodesy) and experts in space technologies[6]. As shown in Table 2, some use-cases were prioritized, along with the necessary spatial resolution, temporal resolution, and signal magnitude, expressed in term of the cumulative geoid error (CGE). To comment on a particular use case, let's take the case of melting of ice sheets. The clause "with separation of glacial isostatic adjustment (GIA)" means that the ongoing movement of land once burdened by ice-age glaciers must also be monitored. This is a very slow effect, which takes place on a secular timescale; on the other side, the ice melting is affected also by seasonal phenomena. Therefore, this use case requires two distinct temporal resolutions, seasonal and secular, and a spatial resolution of 100 to 1,000 km. The magnitude of the signal to be monitored, expressed in geoid height, is expected to be in the range of 1mm for yearly

[6] "Next Generation Gravity Mission", Stefano Cesare and Gianfranco Sechi, Space Technology Library, Vol. 31, 2013; https://link.springer.com/chapter/10.1007/978-1-4614-4541-8_20

variations, much smaller for variations on the secular timescale. Such considerations yield the gravity mission requirements detailed in the subsequent Table 3: for a gravity field retrieved with a monthly frequency, the CGE must be smaller than 0.1mm in the spherical harmonic range between degree 20 and 200. It can be seen from Fig. 4 that GRACE-FO falls short of this requirement, especially at the higher spherical harmonic degree end.

	Description	Spatial resolution	Temporal resolution	Signal magnitude in geoid heights
1	Melting of ice sheets (with separation of glacial isostatic adjustment)	100–1,000 km	Seasonal Secular	0.01–1 mm/year (secular)
2	Non-steric component of sea-level variations at seasonal and shorter time scales	Global to basin level	Inter-annual Secular	0.1 mm/year (secular)
3	Ground water (soil moisture and snow) at larger spatial scales	10–200 km	Hourly Seasonal Secular	0.05–1 cm (seasonal)
4	Post-seismic deformation	10–200 km	Sub-seasonal	1 mm (sub-seasonal)

Table 2: Fields of prioritisation for the NGGM, including the required spatial and temporal resolution and the approximate signal magnitudes.

	Resolution	10000 km	1000 km	200 km	100 km	10 km
	Spherical harmonic degree	$\ell = 2$	$\ell = 20$	$\ell = 100$	$\ell = 200$	$\ell = 2000$
CGE	10 mm			3		
	1 mm	2		4		
	0.1 mm		1			

Table 3: Requirements in terms of maximum cumulative geoid error (CGE) for monthly gravity field retrievals. The numbers in the grey boxes correspond to the use cases represented in Table 2, and the shaded areas on the right mark the spatial resolution range which is not realistically accessible for a monthly gravity field. Note that the spherical harmonic degree here indicated with ℓ corresponds to the index n in the gravity field potential expansion given in the previous Section.

Again from the ESA-funded 2013 study, we read "To satisfy the requirements of the geophysical applications (solid-earth science, glaciology, hydrology, oceanography, atmosphere circulation, etc.), the NGGM must provide the temporal variations of the Earth's gravity field over a long time span (possibly covering a complete solar cycle: ~11 years) with high spatial resolution (comparable to that provided by GOCE) and high temporal resolution (weekly or better), so as to reduce the level of aliasing of the high frequency phenomena found in the time series of the Earth's gravity field variation provided by GRACE, and to improve the separability of the observed geophysical signals. Moreover, the NGGM shall be able to provide the following CGEs from monthly solutions of the Earth gravity field:

- CGE ≤ 0.1 mm at degree 150 (spatial resolution 133 km),
- CGE ≤ 1 mm at degree 200 (spatial resolution 100 km),
- CGE ≤ 10 mm at degree 250 (spatial resolution 80 km).

From the wavelengths of the geopotential spherical harmonics to be monitored, the measurement bandwidth (MBW) of the NGGM has been preliminarily established between

1 and 100 mHz (corresponding to a spatial sampling along the orbit between ~77 and ~7,700 km). The LL-SST (low-low satellite-satellite tracking) is in practice the only observing technique potentially capable of detecting the time variable gravity signal with the required resolution."

The Council of the International Union of Geodesy and Geophysics (IUGG) published in 2015 a study summarizing the desiderata of a large representation of the scientific communities involved in gravity mission proposals[7]. To summarize the received specifications, the authors produced a graph spanning at least three orders of magnitudes of spatial resolution and six orders of magnitudes with respect to the magnitude of the signal to be detected, see Fig. 6. This clearly evidences how strongly the performance requirements suggested for a gravity mission depend on the phenomena it is intended to investigate.

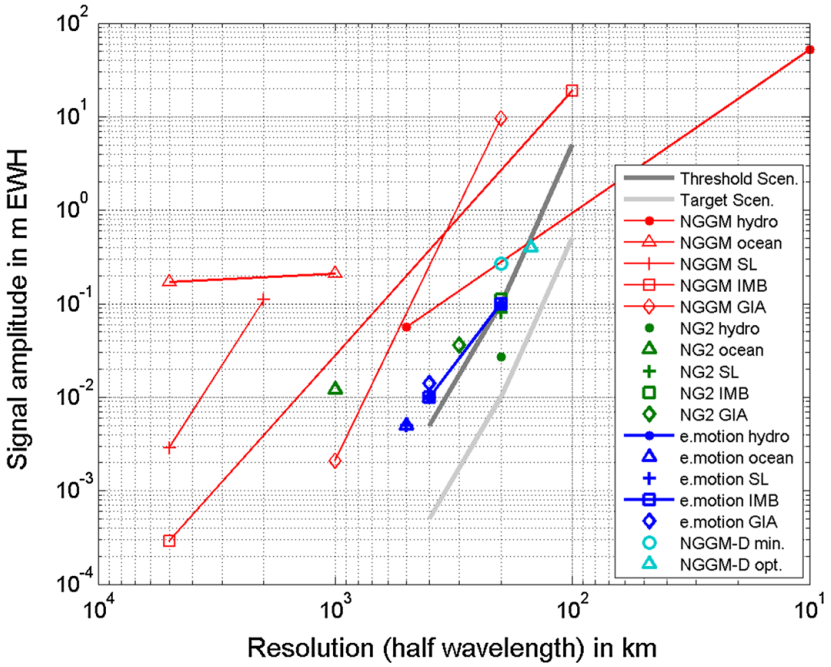

Fig. 6: The coloured lines show the various science requirements derived in previous studies for individual fields of applications. The light and dark grey curves show two scenarios for the consolidated requirements derived in the IUGG 2015 study. SL: sea level; IMB: ice mass balance; GIA: glacial isostatic adjustment. The IUGG document reports in an appendix the table of equivalences between Equivalent Water Height (EWH in meters) of and gravity anomaly (in milliGals), for which an analytical relation is not available.

The IUGG made an effort to translate these requirements in a compact form. From one side, it identified a "threshold scenario", broadly corresponding to significant but not transformative improvements with respect to the present situation. Broadly speaking, the threshold scenario (represented by the dark grey line in Fig. 6) involves a 5x improvement with respect to the current situation. The IUGG proposes also a "target scenario" (show by the clear grey line in Fig. 6), which roughly corresponds to a 50x improvement with respect to the current situation, and whose implementation would allow transformative applications of satellite-based gravimetry. In a compact clause, the IUGG states that "the required target performance in terms of equivalent water height has been identified as 5 cm for monthly fields and 0.5 cm/year for long-term trends at a spatial resolution of 150 km". No attempt is made to identify the necessary technologies: it is only en passant said that while the threshold scenario can conceivably be attained by improving existing techniques, the target one will likely require a completely new set of technologies; no reference to atomic interferometry as a possible technology for future gravity mission is made.

[7] "Science and User Needs for Observing Global Mass Transport to Understand Global Change and to Benefit Society", R. Pail et al., Surv. Geophys. 36, 2015; https://link.springer.com/article/10.1007/s10712-015-9348-9

The IUGG document provides several examples of the improvements enabled by the threshold and target scenarios. In Fig. 7 we show for example the improved mapping of the mass variation in west Antarctica, while in Fig. 8 it is shown how the two scenarios would allow monitoring even weaker earthquakes than now possible.

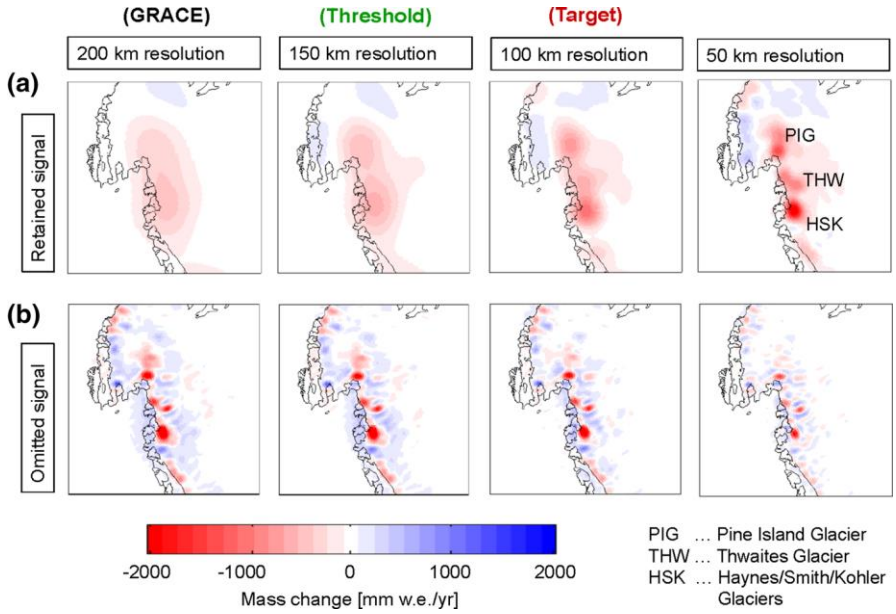

Fig. 7: Illustration of ice sheet mass change signal content and signal omission for different spatial resolutions. For this simulation, elevation trends from ICESat laser altimetry are used as a proxy for the spatial patterns and spectral properties of the actual mass change signal. (a) Signal retained by different spatial resolutions for the example of the Amundsen Sea Sector of West Antarctica. (b) Signal omitted due to the respective resolution limits. The sum of (a) and (b) in each column gives the full signal. The first three columns illustrate the resolution at which the three scenarios "GRACE", "Threshold" and "Target" may resolve long-term trends with a 5 cm EWH/yr accuracy. [Text reported verbatim from IUGG 2015].

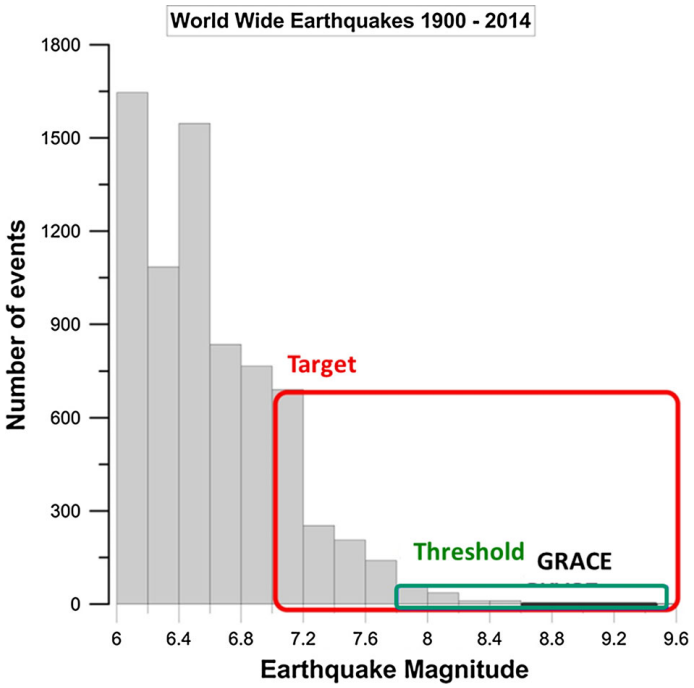

Fig. 8: Earthquake monitoring from space. Grace allows detecting quakes of magnitude larger than 8.6, the implementation of the "threshold" scenario would allow observing earthquakes stronger than 7.8, while the "target" scenario would allow observing events stronger than 7.0.

4 Evolution of existing technologies

4.1 GRACE-like concept

In a 2020 paper, ESA stated that "Scientific objectives for Next Generation Gravity Missions are the measurement of the geoid with an accuracy of 1mm at a spatial resolution of 500km every 3 days and 150km every 10 days" [8]. The paper describes the likely technological improvement necessary to attain this scientific objective. In the conclusive remarks, they state that "In the near future, concepts based on laser ranging between low-flying pairs of satellites offer the most mature solution for measuring the time-variable gravity field. The required technological and scientific developments are on-going and it seems theoretically to be feasible to implement such a mission within the next decade". It is also added that "For the far future, CAI (cold atom interferometry) offers an interesting perspective for measuring the time-variable gravity field as well as the mean gravity field with improved measurement system performance".

In Fig. 9 the working principles of GRACE-like gravity mission is briefly recalled. Gravity is obtained by measuring the variations in the distance between the satellites, which have on-board accelerometers to measure non-gravitational pull (due e.g. to atmospheric drag, radiation pressure, etc), and compensate it by driving the attitude and orbit control system (AOCS). A microwave link between the satellites ensures a ~10μm precision in the distance measure. Grace FO has also laser ranging as technology demonstrator, which is planned to increase the distance measurement precision by an order of magnitude. This would allow reducing the cumulative geoid error from ~1cm to 1mm, or equivalently improving the accuracy of the gravity anomaly measurement from 1mGal to 100μGal.

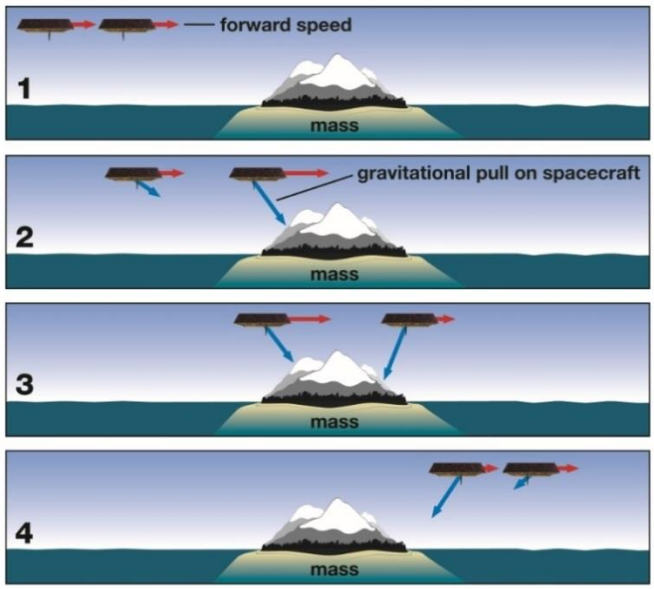

Fig. 9: Representation of the working principle of a GRACE-like gravity mission. The gravitational effect of the mountains and of the ice covering them is translated into the distance between the two orbiting satellites.

The emerging consensus for a Grace-like Next Generation Gravity Mission to be flown in the next ~10 years foresees a constellation of several pairs of satellites, at a lower orbit (~350km) and at a smaller distance (~100km). A favourite configuration is the so called "Bender", shown in Fig. 10. Laser interferometry will be used to improve inter-satellite distance measurements, precise satellite location will be ensured not only by GNSS satellite-to-satellite tracking but also by laser ranging from ground stations, and on-board accelerometers will still be used to measure non-gravitational pull, as shown in Fig. 11.

[8] "ESA's next-generation gravity mission concepts", R. Haagmans et al., Rendiconti Lincei. Scienze Fisiche e Naturali, Rend. Fis. Acc. Lincei, 2020 ; https://link.springer.com/article/10.1007/s12210-020-00875-0

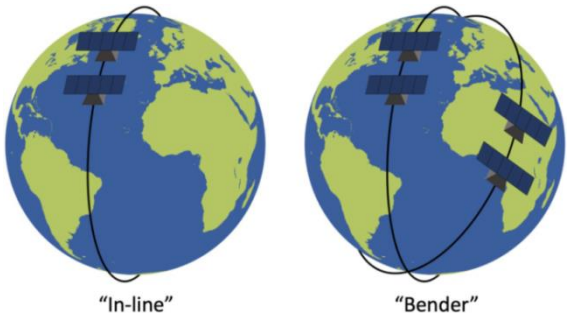

Fig. 10: Single-pair and two-pairs satellite constellations for future GRACE-like gravity missions.

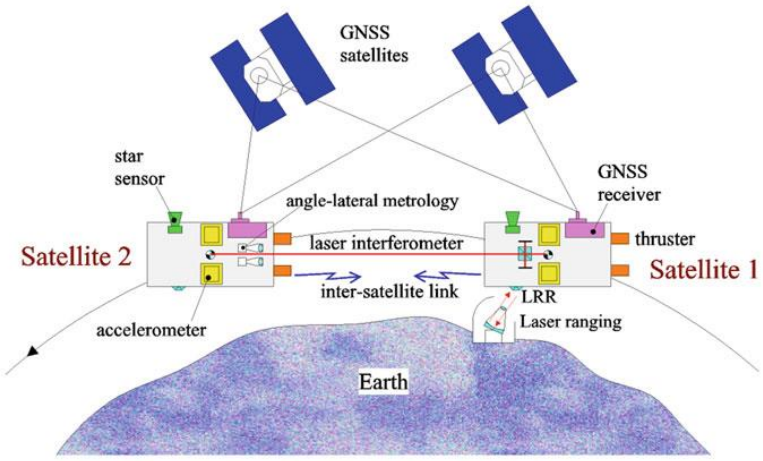

Fig. 11: In a next generation GRACE-like gravity mission laser interferometry would be used to improve the precision of the inter-satellite distance measurement.

4.2 GOCE-like concept

Gravity gradiometry measures the variation of acceleration by using pairs of accelerometers slightly displaced in space. The driving idea is that if the accelerometers are identical the common-source disturbances affecting the gravity signal will be recorded in in the same way by the two devices, and will therefore disappear from the differential signal. GOCE gradiometer is formed by three pairs of tree-axis accelerometers, each one providing the three linear and the three angular components of the acceleration. From the differences between the accelerations, the six different components of the symmetric gravity gradient tensor can be obtained. The derivation is however affected by several factors: for example, an extremely accurate calibration of the accelerometers is needed, and the angular position and motion of the satellite needs to be known with great accuracy. To this aim, the rotation angles and their time derivatives are obtained both from the gradiometer itself and from additional equipment on-board the satellite, such as a star sensor. The components of the gravity gradient tensor are therefore calculated, and additional elaborations yield a gravity anomaly map, as shown in Fig. 12. The acceleration $\boldsymbol{a}$ measured by each one of the accelerometers, located in $\boldsymbol{r}$, is given by[9]

$$\boldsymbol{a} = -\boldsymbol{V} \cdot \boldsymbol{r} + \dot{\boldsymbol{\omega}} \times \boldsymbol{r} + \boldsymbol{\omega} \times (\boldsymbol{\omega} \times \boldsymbol{r})$$

This is a highly idealized expression, which for example does not take into account the sensor bias and scale factor drifts, its misalignment, the displacement of its centre of

[9] "GOCE gradiometer – a guide for users", C. Stummer et al, FGS workshop, 2008; http://www.fs.wettzell.de/veranstaltungen/fgs/workshop2008/poster/FGS2008_Stummer.pdf

mass, etc. The first term in the second hand side is the linear acceleration experienced by the sensors because of the gravity gradient tensor $\boldsymbol{V}$, the second is the linear acceleration induced by the satellite angular acceleration $\dot{\boldsymbol{\omega}}$, and the third is the acceleration induced on the sensor by the satellite angular rotation $\boldsymbol{\omega}$. All the components of the acceleration differences can be deduced by this formula. For example,

$$a_{1,z} - a_{4,z} = L_x\left(-V_{zx} - \dot{\omega}_y + \omega_x\omega_z\right)$$

So the gravity gradient component V_{zx} can be deduced from the differential signal $a_{1,z} - a_{4,z}$ given by the instrument (here the subscripts 1 and 4 refer to two particular accelerometers, the ones displaced along the x axis in Fig. 12), provided that the angular acceleration component $\dot{\omega}_y$ and the angular rates ω_x and ω_z are known. These are usually obtained by combining the output of the gradiometer accelerometers with those of the star tracking system. Note that minimal variations in the distance between the accelerometer pairs (L_x in this particular case) must be ensured. In GOCE, the distance is 50cm and its variation is of the order of 1% of an Å, over a time interval of three minutes. A scheme of the instrument is shown in Fig. 13, with its noise properties.

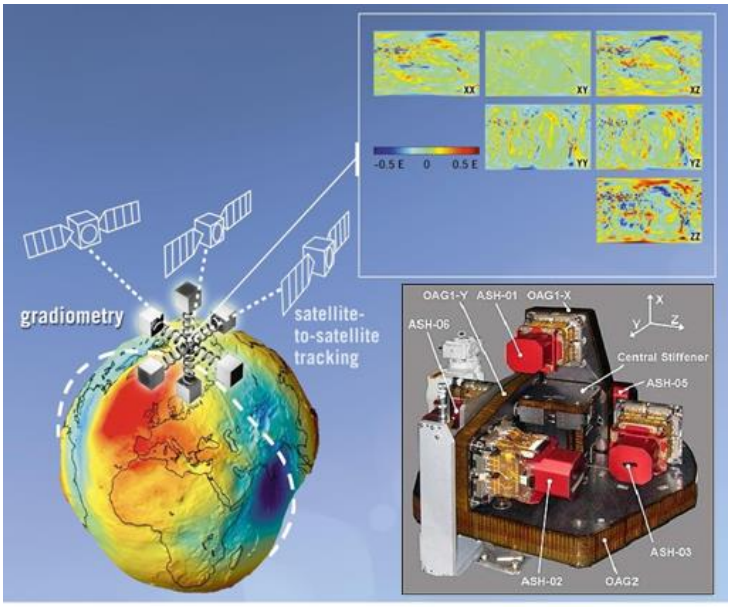

Fig. 12: GOCE gravity gradiometer, the six component of the symmetric gravity tensor, and the geoid[10].

To better appreciate the performance of GOCE, let us compare them with the ones of a Superconducting Gravity Gradiometers which is being developed by the Department of Physics in the University of Maryland (Gravitation Experiment Group, see http://www.physics.umd.edu/GRE/SGGs.htm). They report that "several versions of the superconducting gravity gradiometer (SGG) have been developed. A three-axis in-line component SGG with a baseline of 19 cm, developed with NASA support, reached a performance level of $2{\cdot}10^{-11}$ s^{-2} $Hz^{-1/2}$ in the laboratory, which is three orders of magnitude more sensitive than the demonstrated sensitivities of atom gravity gradiometers to date." The reported prototype sensitivity of $2{\cdot}10^{-11}$ s^{-2} $Hz^{-1/2}$ corresponds to GOCE performance of 20 mE $Hz^{-1/2}$, given that $1E=10^{-9}$ s^{-2} and thus $10mE = 10^{-11}$ s^{-2}. Current portable atomic gravity gradiometers have sensitivities which are approximately three orders of magnitude lower, i.e. ~10E $Hz^{-1/2}$. To give an idea of their possible applications, a 1Eötvös gradiometer can resolve a 10cm void at a depth of 1m. An instrument with a sensitivity of 10E could be employed to detect relatively large underground features, and therefore can be of interest to civil engineering.

[10] "Goce gravity mission", ESA publication office, 2006; http://www.esa.int/esapub/br/br209/br209.pdf

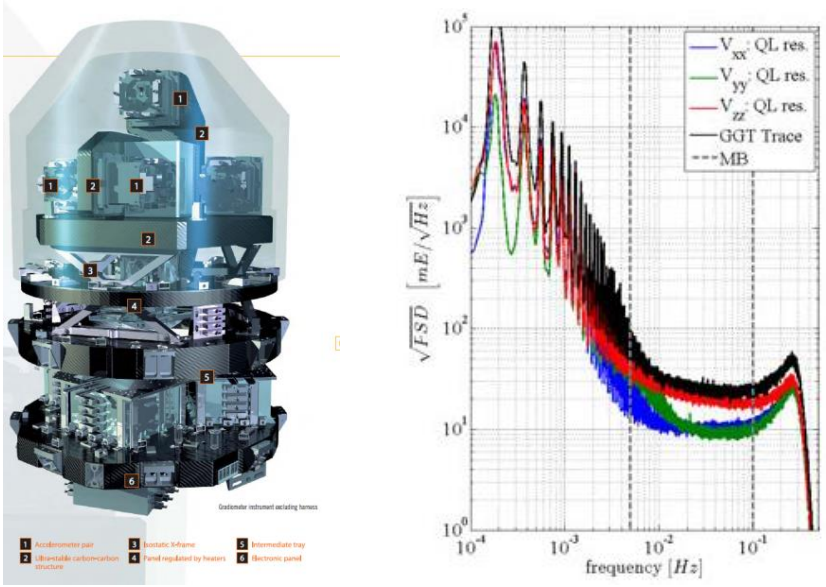

Fig. 13: GOCE gravity gradiometer (180Kg, 100W) and its noise characteristics, determined by the electrostatic accelerometers it employs (see next subsection). The noise amplitude exhibits a flat spectral density of 10 to 20 mE $Hz^{-1/2}$ in the frequency range 2 to100 mHz, and a large increase below 2mHz. More in detail, the gravity gradient components Vxx and Vyy reach a noise level of about 10 mE $Hz^{-1/2}$, while for Vzz and Vxz we have ~20mE $Hz^{-1/2}$ [11].

4.3 Electrostatic accelerometers

All the gravity missions described until now used electrostatic accelerometers manufactured by Onera, with the following sensitivities

- CHAMP mission, 2000-2010: "Star" accelerometer, ~10^{-9} m/s^2
- GRACE mission, 2002-2017: "SuperStar" accelerometer, ~10^{-10} m/s^2
- GOCE mission, 2009-2013: "Gradio" accelerometer, ~10^{-12} m/s^2
- Grace FO 2018→: evolved SuperStar, with similar performances

To give a concrete example, in Fig. 14 it is shown the SuperStar accelerometer. The acceleration (linear and angular components along the three axes) is deduced by the electrostatic fields needed to keep a proof mass suspended inside a case. The distances between the mass and the case are measured by electrodes, whose signal drives the fields.

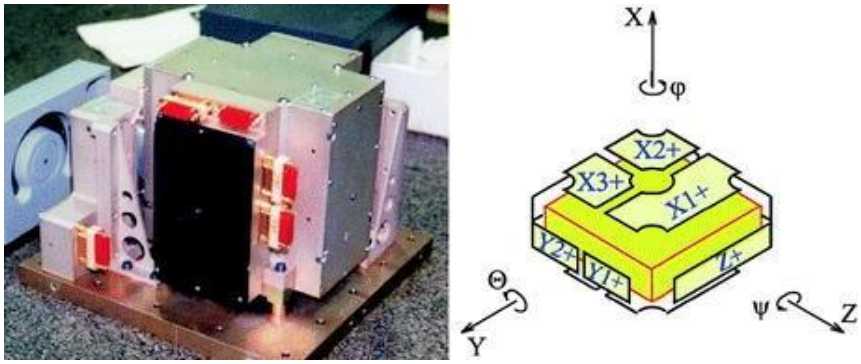

Fig. 14: Superstar electrostatic accelerometer by Onera. The proof mass is a 40x40x10mm gold-coated titan cube of 72g. In GOCE, the accelerometer proof mass is a platinum-rhodium alloy, 40x40x10mm, 320grams[12].

[11] "GOCE gravitational gradiometry", Reiner Rummel, Weiyong Yi, and Claudia Stummer, Journal of Geodesy Vol. 85, No. 777, 2011; https://link.springer.com/article/10.1007/s00190-011-0500-0

[12] "The GRACE Gravity Sensor System", Björn Frommknecht et al., System Earth via Geodetic-Geophysical Space Techniques, 105-118, 2010; https://link.springer.com/chapter/10.1007/978-3-642-10228-8_9

The noise properties of the ES accelerometers used in the GRACE Follow-On mission and in the GOCE mission are represented in Fig. 15. It can be noted that in both cases the total noise increases at low frequencies (i.e. below ~mHz). It can be noted that the figure of merit of the Gradio accelerometers used in GOCE is almost an order of magnitude better than the one of the accelerometers used for GRACE-FO. Gradio is therefore often taken as a reference against which define the requirements for new accelerometers.

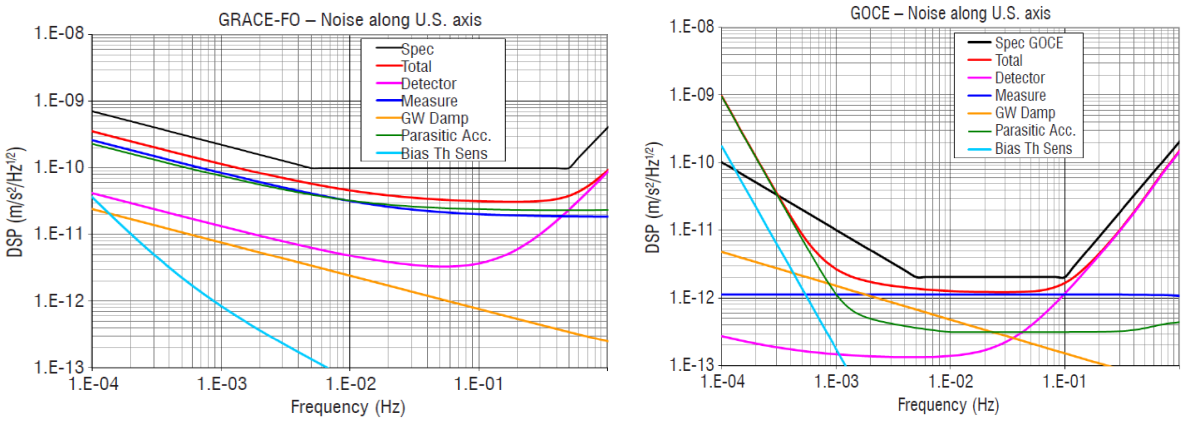

Fig. 15: Noise properties of the Onera electrostatic accelerometers used in GRACE-FO and in GOCE[13].

In particular, the following requirements have been identified for Next Generation Gravity Mission accelerometers:

- Noise level between $1.5 \cdot 10^{-12}$ m/s^2/Hz$^{1/2}$ and $4 \cdot 10^{-11}$ m/s^2/Hz$^{1/2}$ over 1–10mHz;
- Improvement of the low-frequency noise (below 1mHz) with respect to GOCE;
- Identical performance along the three directions;
- Accurate angular acceleration to complement star trackers for the attitude control

Onera has already developed a prototype, called MicroStar, which satisfies the above specifications, see Fig. 16. It weighs 0.98kg, with dimensions of 90x90x70mm, and 2W power requirements. The proof mass is 18gr, and the gap dimension can be selected from 50µm to 300µm, depending on the mission requirements.

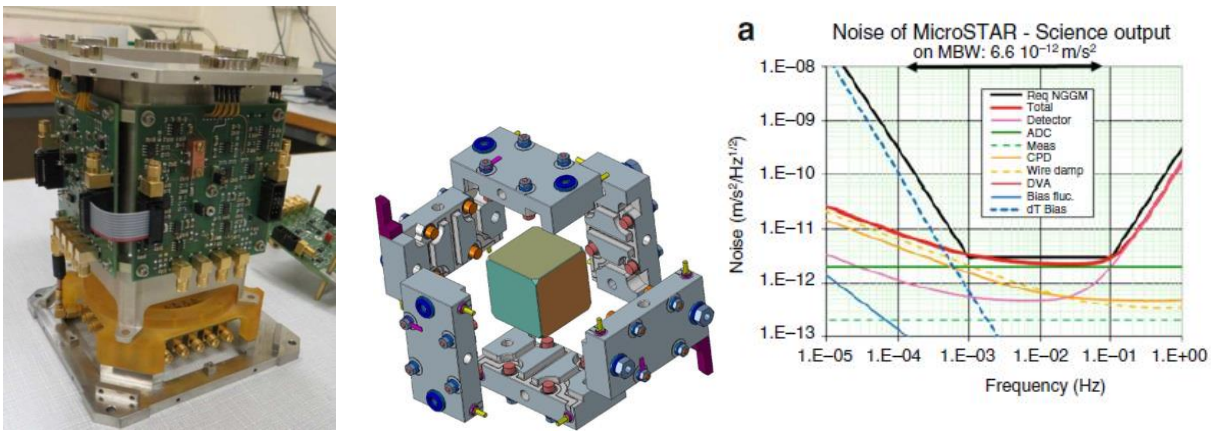

Fig. 16: Onera MicroStar accelerometer[14].

[13] "Gravitation and Geodesy with Inertial Sensors, from Ground to Space", P. Touboul et al., Journal of aerospace Lab, Issue 12, 2016;
http://www.aerospacelab-journal.org/sites/www.aerospacelab-journal.org/files/AL12-11.pdf

[14] "A new generation of ultra-sensitive electrostatic accelerometers for GRACE Follow-on and towards the next Generation gravity missions", B. Christophe et al., Acta Astronautica 117, 1-7, 2015;
https://www.sciencedirect.com/science/article/abs/pii/S0094576515002660

We conclude this section with a figure representing the surface gravity magnitude of several geophysical phenomena, and a brief overview of the main techniques that can be used to monitor them.

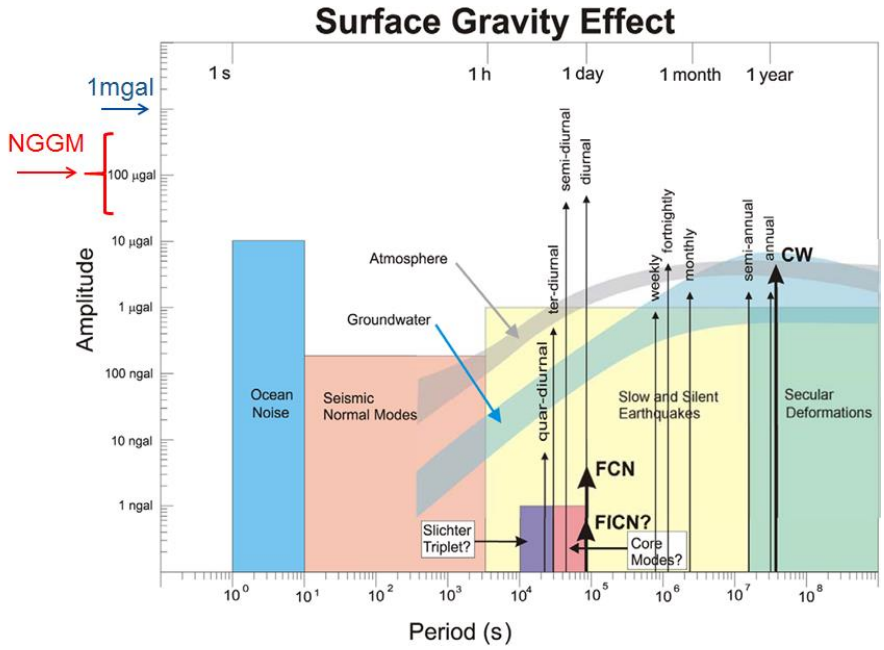

Fig. 17: Gravity impact of several geophysical phenomena[15]

Current satellite-based gravity measurement reaches sensitivity of ~1mGal, and next generation gravity mission aim at improvements in the range of 5x to 50x, so that sensitivities in the 20-200µGal interval can be reached. Note from the following Table 4 that on-ground instruments (even commercial ones) can deliver much higher sensitivities. The best gravity measurement has been obtained with the 8-meters cold atom fountain at Stanford, which reaches sub-nanogal sensitivity. A second thing to be noted is that satellite-based gravity missions have a typical field retrieval time of a month or so. This means that phenomena which take place over faster time scales and are strong enough to be detectable would need an accurate modelling, to avoid signal aliasing. If future satellite gravity observation missions were to reach sensitivities better that ~10µgal, Atmospheric-Oceanic (AO) noise in particular would need to be taken into account.

	Detectable gravity anomalies (gal)	Accuracy ($\delta g/g$)	Measurement duration
Current satellite gravimetry	1mgal	10^{-6}	Seasonal
Next Generation Gravity Missions	50µgal - 500µgal	10^{-7}	Sub-seasonal
Falling corner cube absolute gravimeter	~ 1 µgal	10^{-9}	Days/hours
CAI portable gravimeter (muQuans)	~ 1 µgal	10^{-9}	~1hour
Stanford ~10m fountain CAI accelerometer	~ 1 ngal	10^{-12} 10^{-13}	Single-shot ~1hour

Table 4: order of magnitude of the gravity measurements capability of (i) current satellite gravity missions (ii) Next generation satellite gravity missions (iii) high-end standard reference commercial absolute instrument (iv) portable CAI gravimeter, and (v) non-portable CAI gravimeter.

[15] "The measurement of surface gravity", David Crossley et al., Reports on Progress in Physics, Vol. 76, No. 046101, 2013; https://iopscience.iop.org/article/10.1088/0034-4885/76/4/046101

5 Cold Atom Interferometry for future gravity missions

There are several different ways in which cold atom interferometry can be usefully employed in the context of a satellite gravity mission for Earth observation. As we have seen, accelerometers play an essential role in any such mission, and CAI-based accelerometers have peculiar advantages over conventional ones: in particular, a flat noise spectrum. Hybrid accelerometers which combine the properties of classical and atomic interferometric systems are therefore being studied, which could be used in the context of a future GRACE-like mission, to measure non-gravitational pull. A second idea is to correlate the signal of two CAI accelerometers placed in two distinct satellites by means of a laser interferometric link. Such a mission has some elements of GRACE (the use of a pair of satellites) and of GOCE (a component of the gravity tensor will actually be measured), since it would yield a gravity gradiometer with an extremely long baseline. A third possibility, which seems to have elicited the interest of several research groups, is to develop a CAI-based gravity gradiometer, to be flown in a satellite with the aim of improving the GOCE performances. In the following subsections we review the status of these lines of activity.

5.1 Hybrid electrostatic – CAI accelerometer

Onera is working with ESA funding on a hybrid accelerometer[16], composed of an electrostatic accelerometer and a cold atom interferometry accelerometer. Indeed, as shown in the previous section (see e.g. Fig. 16) electrostatic accelerometers have reached extremely high sensitivity level, but are intrinsically affected by a non-flat noise response and bias drift. On the other side, a CAI-based accelerometer is characterized by white noise and very good bias stability. Onera has been developing and characterizing a hybrid system where the proof mass of the electrostatic accelerometer is the Raman mirror of the atom interferometer. The CAI system measures atomic acceleration relative to proof mass acceleration, or conversely the acceleration of the proof mass with respect to the atoms inside the atomic interferometer, which constitute an inertial system of reference.

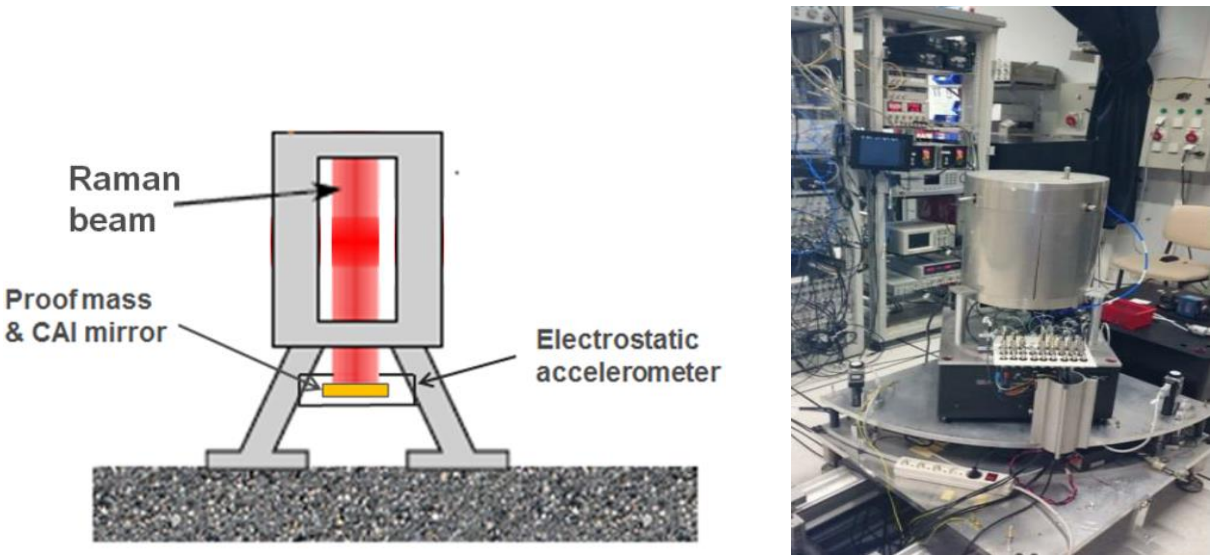

Fig. 18: concept and prototype of hybrid accelerometer

[16] "Status of Development of the Future Accelerometers for Next Generation Gravity Missions", B. Christophe et al., International Symposium on Advancing Geodesy in a Changing World, pp. 85-89, 2018; https://link.springer.com/chapter/10.1007/1345_2018_42

A feedback loop can therefore be implemented, by which the signal coming from the CAI accelerometer is used to drive the field keeping suspended the proof mass in such a way that all the low-frequency noise components (e.g. vibrations, thermal drifts) are suppressed in the electrostatic accelerometer. In Fig. 19 it is shown how the disturbances introduce by a purposely-introduced sinusoidal vertical excitation can be suppressed, so that once the right feedback is found (red line) the atomic signal falls back to the region where it was before the excitation was applied (green line)

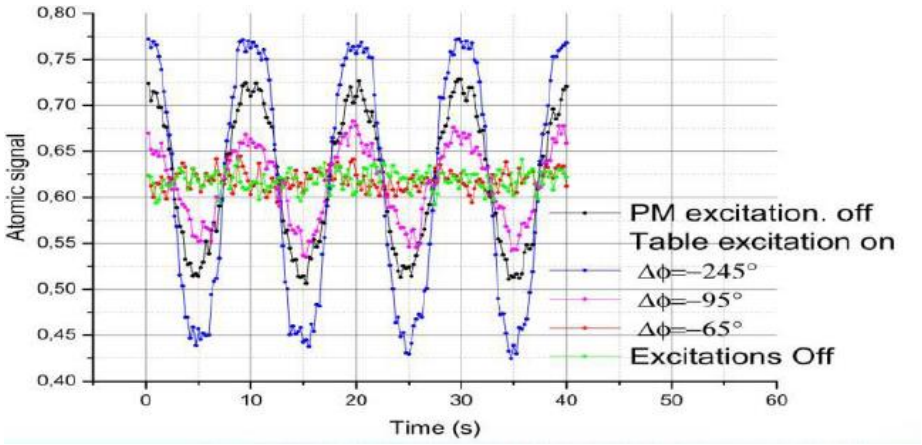

Fig. 19: suppression of vertical oscillations in a hybrid accelerometer.

In Fig. 20 it is shown how the noise spectra of the hybrid system changes. The low frequency noise of the composed device is flat, instead of rising as the black one of the ES accelerometer alone.

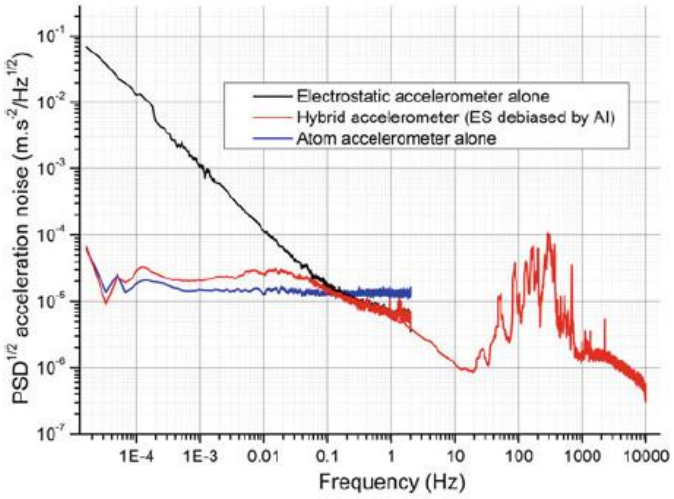

Fig. 20: noise spectrum of the hybrid accelerometer

A comparison of Fig. 20 with Fig. 16 shows however that this constitutes just a proof-of principle demonstration. The low-frequency flat noise spectrum of the hybrid system has a noise level of $\sim 10^{-4}/10^{-5}$ $ms^{-2}/HZ^{1/2}$, to be compared with a requirement of $\sim 10^{-11}/10^{-12}$, if the noise spectrum of an actual ES accelerometer such as the microStar is to be made flat. However, it should be taken into account that performances at 0g are expected to be much better than at 1g, both because of the longer interrogation time in the atomic interferometer, and because the proof-mass would be suspended under the optimized conditions of a 0-Volt field, since no static bias field would be required to keep the mass suspended in the absence of gravity. Future plans include the test of compensation of static and dynamic rotations. The plan of the work can be found e.g. in an ESA presentation, where further details about the instrument have also been presented, see Fig. 21.

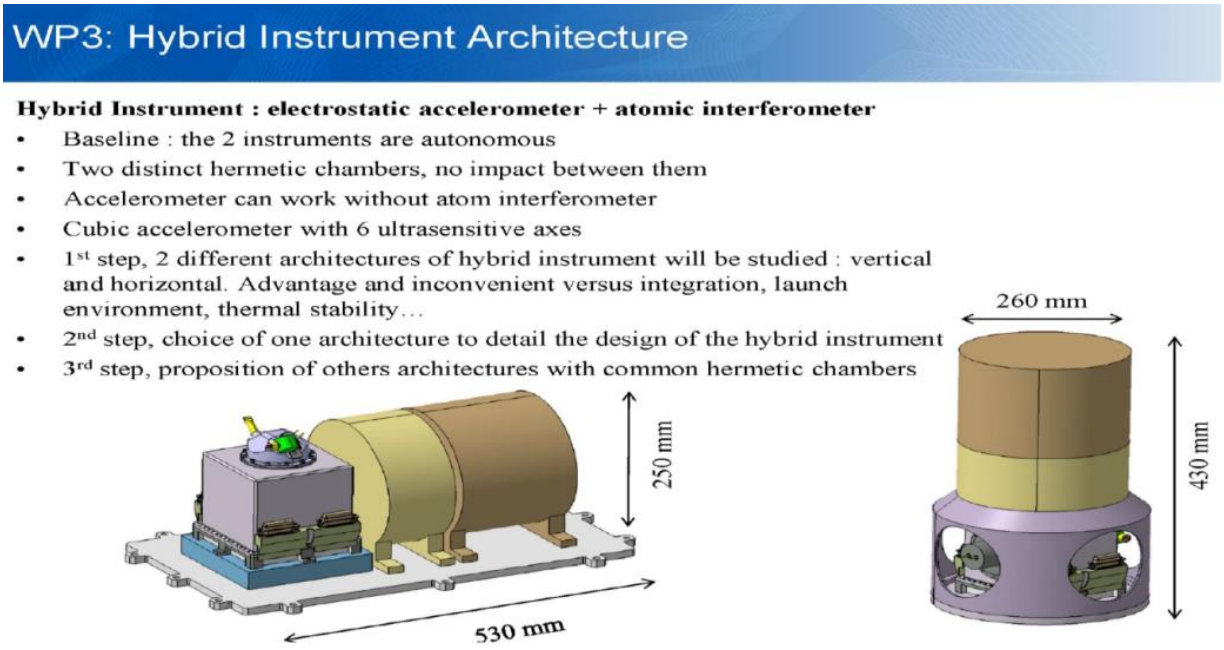

Fig. 21: architecture of the hybrid instrument; work carried on thanks to ESA funding for Onera hybrid accelerometers. [17]

The impact that a hybrid accelerometer like the one being developed by Onera may have in a GRACE-like mission has been explored in terms of the improvement in the geoid accuracy[18] by a group composed by researchers form Technische Universität München, ONERA, Université Paris-Saclay, and RHEA for ESA. In Fig. 22 we show how different performance assumptions (left-hand side) impact on the geoid accuracy (right-hand side).

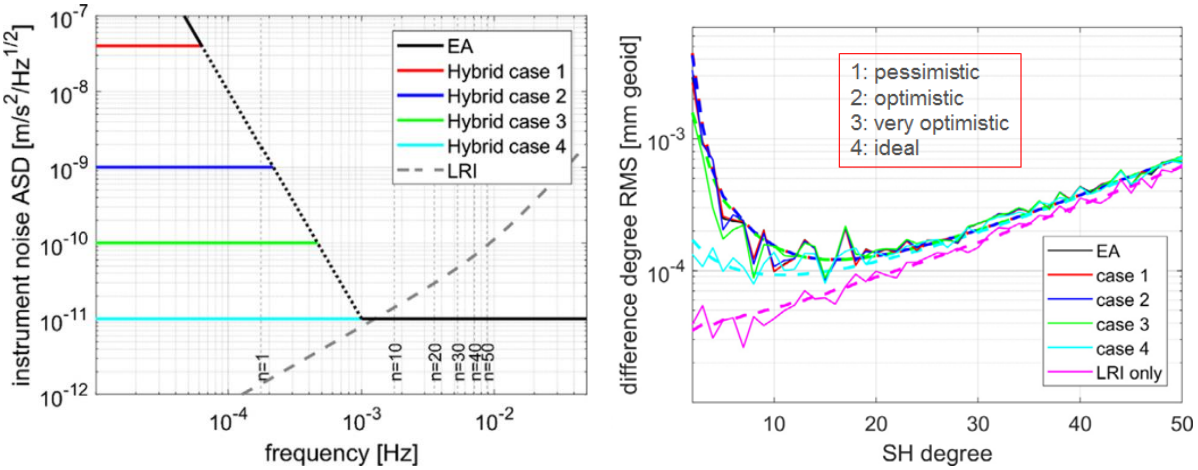

Fig. 22: Performances assumption on the hybrid accelerometers and simulated improvement on geoid at different spherical harmonic degrees. LRI means laser ranging interferometer. The noise associated with LRI sets the ultimate limit for the geoid accuracy.

[17] "Cold Atom Interferometers for Future Inertial Sensors and Gradiometers", O. Carraz, Alpbach Summer School presentation, 2019; https://www.summerschoolalpbach.at/docs/2019/lectures/Carraz_QT_ESA.pdf

[18] "Impact of a novel hybrid accelerometer on satellite gravimetry performance", P. Abrykosov et al., Advances in Space Research 63, 3235–3248, 2019; https://hal.archives-ouvertes.fr/hal-02315304/document

It is apparent that for the hybrid system to yield an appreciable improvement, a completely flat noise spectrum is necessary. This is acknowledged by the authors, which write "while a low CAI performance (10^{-8} to 10^{-9} m/s^2/Hz$^{1/2}$) does not lead to any gains compared to a stand-alone EA, a sufficiently high one (10^{-11} m/s^2/Hz$^{1/2}$) may improve the retrieval performance by over one order of magnitude". This ideal flat noise spectrum is, in their own assessment, more than very optimistic. Other factors come also into play: for example "the accelerometer performance seems to play a less prominent role if the overall observation geometry is improved as it is the case for a Bender-type mission", and "the impact of the accelerometer measurements diminishes further when temporal variations of the gravity field are introduced, pointing out the need for proper de-aliasing techniques". This implies that, even if the low-frequency noise component of the accelerometer is improved by several order of magnitude, the impact in a fully-simulated mission context can be much less significant than expected. In particular, a perfectly flat noise spectrum would bring an improvement only in the long wavelength spectrum of the gravity field (i.e. spherical harmonic degree lower than ~20), which are of interest for global mass transport studies but would not improve the system spatial resolution.

There is an additional element which the authors bring to the attention of the reader, when they write that "in order to maximize [the hybrid accelerometer's] potential, the application of de-aliasing techniques, especially for non-tidal AO signals and the tidal component of the gravity field, shall be a decisive factor. This is a reasonable demand for the upcoming decades, as first results by Daras and Pail (2017) as well as Hauk and Pail (2018) have shown". This statement points to the fact that deploying on a satellite a better instrument (in this case, one with lower low-frequency noise) is not per se a guarantee of better gravity measurements. As can be seen in Fig. 23, an improvement of the field retrieved performance with respect to GRACE and GOCE requires a very accurate modelling of several phenomena which occur on fast time scales and therefore induce aliasing noise disturbances on the retrieved field.

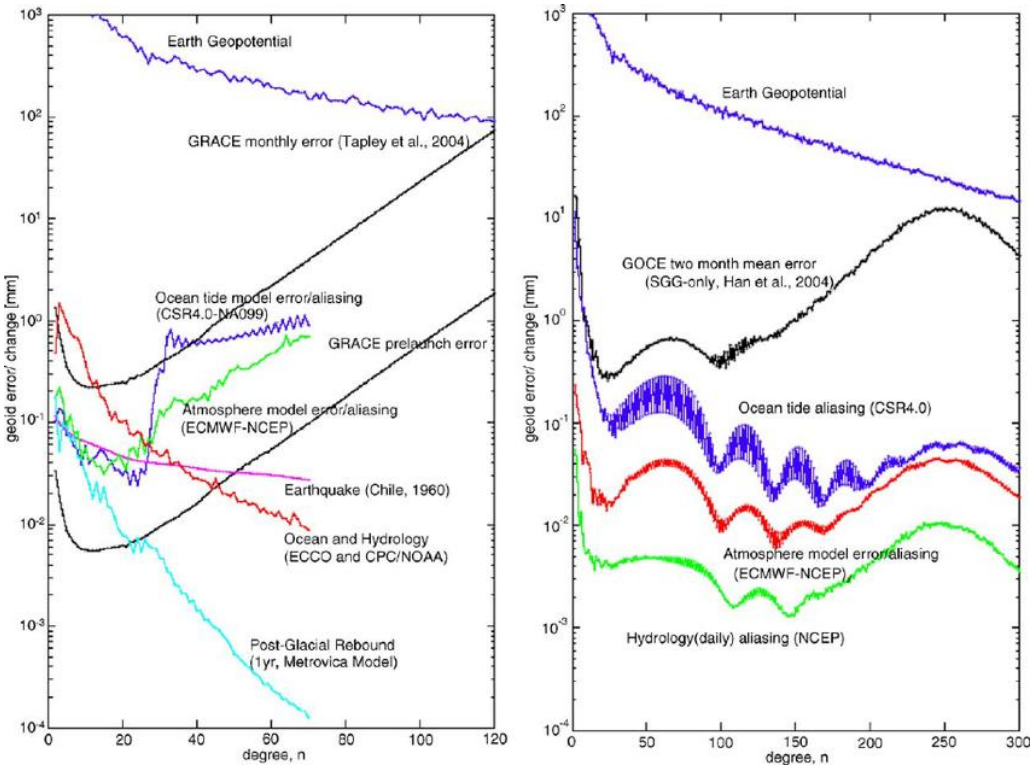

Fig. 23: Magnitudes of different source of errors affecting GRACE and GOCE measurements, at different spherical harmonic degrees.[19]

[19] "The gravity field and the Global Geodetic Observing System GGOS", Journal of Geodynamics Vol. 40, No. 4-5, 387-393, 2005;
https://www.sciencedirect.com/science/article/abs/pii/S0264370705000700?via%3Dihub

5.2 Correlated CAI accelerometers

GRICE (Gradiométrie à Interféromètres quantiques Corrélés pour l'Espace) is an assessment study by the French space agency CNES, whose concept occupies a middle space between GRACE and GOCE. As in GRACE, we have a pair of spaceships connected by a laser link; as in GOCE, the gravity gradient is actually measured. Since each satellite hosts an accelerometer, the gravity gradiometer baseline is of the order of ~100km instead of the GOCE 50cm. This would increase the sensitivity of the instrument by several orders of magnitudes. In addition, atomic interferometry is exploited to obtain a gravity gradient measurement insensitive from the non-gravitational forces acting on the satellites. GRICE is assumed to be a 5 years mission, and it is forecasted to produce a gravity field map with a spatial resolution of 100km and a temporal resolution of 10 days.

The system is represented in Fig. 24: two satellites on a polar orbit at ~370km height carry a cold atom accelerometer each, and the distance between the reference mirrors of the two accelerometers is measured via a laser link, so that a correlated differential acceleration measurement is obtained.

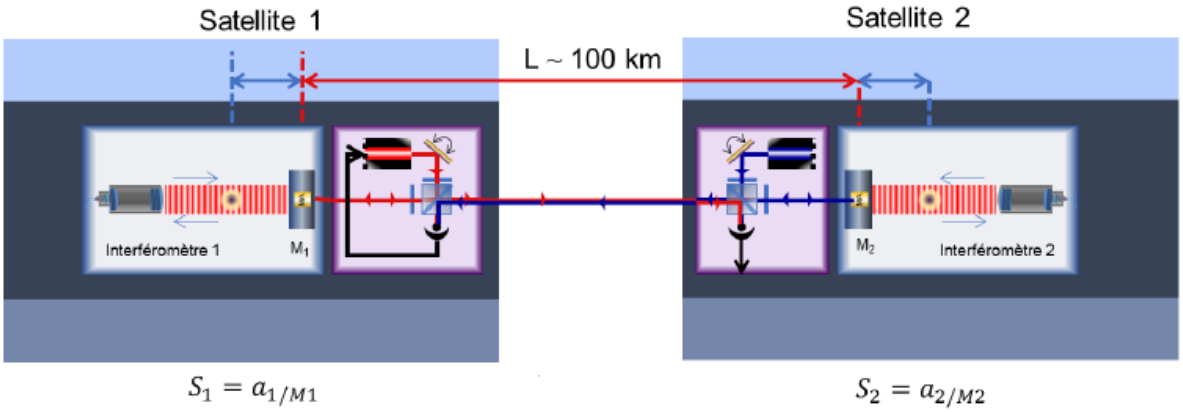

Fig. 24: Gravity gradient measurement concept in GRICE[20]. Having called x the axis connecting the satellites, the two CAI accelerometers measure the x component of the accelerations of the atoms inside the satellites, with respect to the reference mirrors M1 and M2.

The signal S_1 from the first CAI accelerometer gives the acceleration of the atoms in satellite 1 with respect to mirror 1, while the signal S_2 from the second CAI accelerometer gives the acceleration of the atoms in satellite 2 with respect to mirror 2. By taking the second derivative of the satellite distance L, measured by means of a laser interferometric system, we obtain the acceleration of mirror 1 with respect to mirror 2. The variation of the x components of the acceleration along the x axis is given by:

$$\frac{\partial a_x}{\partial x} = \frac{1}{L}\left(S_1 - S_2 + \ddot{L}\right) = \frac{1}{L}\left[(a_1 - a_{M1}) - (a_2 - a_{M2}) + (a_{M1} - a_{M2})\right] = \frac{1}{L}(a_1 - a_2)$$

It is important to note that non-gravitational forces such as the atmospheric drag which acts on the satellites (and therefore on the mirrors) do not affect the accelerations of the cold atoms, which are the only one contributing to the above formula. Using CAI accelerometers therefore allows eliminating in a very natural way non-gravitational pull effects. However, in the proposed architecture only a pair of accelerometers is used, each of them measuring only one acceleration component: consequently, only one component of the gravity field gradient can be retrieved.

[20] "Correlated atom accelerometers for mapping the Earth gravity field from Space", T. Lévèque et al., Proceedings Volume 11180, International Conference on Space Optics — ICSO 2018, 111800W, 2019; https://www.spiedigitallibrary.org/conference-proceedings-of-spie/11180/111800W/Correlated-atom-accelerometers-for-mapping-the-Earth-gravity-field-from/10.1117/12.2535951.full?SSO=1

The following Table 5 summarizes the characteristics of the CAI accelerometers and their performance. Note that to reach an acceleration sensitivity of $6 \cdot 10^{-10}$ $ms^{-2}Hz^{-1/2}$ the atoms must be cooled to 50p°K: to give a comparison, the most recent experiments performed on the ISS by the Cold Atom Laboratory demonstrated a BEC condensate with a temperature of 17n°K, while in the Maius sounding rocket experiment a BEC at 100n°K was obtained[21,22].

Parameter	*Notation*	*Value*	*Unit*
Interaction time	T	0,5	s
Contrast	C	0,81	-
Preparation time	t_{prep}	1	s
Measurement cycle duration	t_c	2	s
Detected atom number	N_{det}	1×10^6	-
Atomic cloud temperature	T	5×10^{-11}	K
Initial size of the atomic cloud	σ_r	1×10^{-4}	m
Accelerometer sensitivity	σ_a	6×10^{-10}	$m.s^{-2}. Hz^{-1/2}$

Table 5: specs and performance of the CAI accelerometers for GRICE

The gravity gradient sensitivity is determined, also by the properties of the laser link. The overall sensitivity is represented by the blue line in Fig. 25. It can be noted that the system is theoretically three orders of magnitude more sensitive than GOCE, and is not affected by the low-frequency increase of noise. As can be seen in Fig. 13 (and later on in Fig. 27), the noise in GOCE is ~10-30 mE $Hz^{-1/2}$ (=$1\text{-}3 \cdot 10^{-11}$ $s^{-2}Hz^{-1/2}$), and steeply increases below 1mHz: however, it must be stressed that from its 6 accelerometers all the components of the gravity gradient tensor can be obtained.

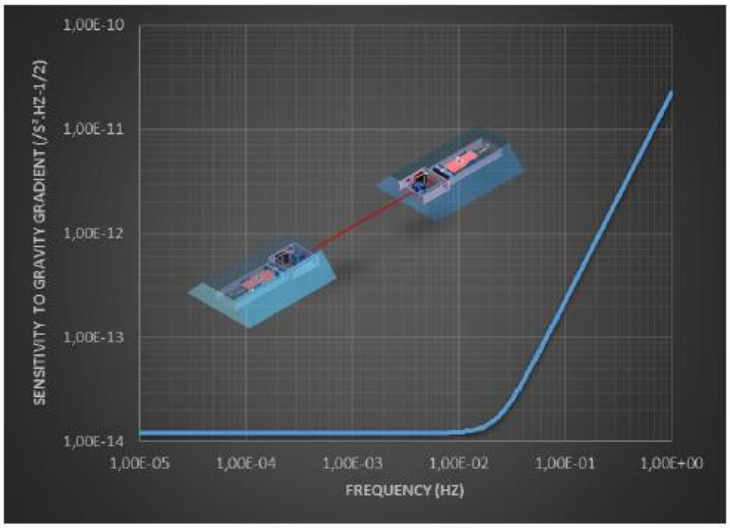

Fig. 25: GRICE expected sensitivity to gravity gradient.

GRICE has been devised to obtain a better spatial resolution of the temporal variations of the high harmonics of the Earth gravity field. To assess to which extent this objective can be attained, its proponents acknowledge that it is still necessary to (1) simulate the gravity field recovery (2) develop specific data processing methodologies (3) validate the instrument sensitivity and (4) assess impact of mission parameters.

[21] "Observation of Bose–Einstein condensates in an Earth-orbiting research lab", David C. Aveline et al., Nature, Vol. 582, pages 193–197, 2020; https://www.nature.com/articles/s41586-020-2346-1 https://www.researchgate.net/publication/342102533_Observation_of_Bose-Einstein_condensates_in_an_Earth-orbiting_research_lab

[22] "Space-borne Bose-Einstein condensation for precision interferometry", D. Becker et al., Nature volume 562, pages 391–395, 2018; https://www.nature.com/articles/s41586-018-0605-1 https://arxiv.org/pdf/1806.06679.pdf

5.3 Satellite-based CAI gravity gradiometers

As we have seen in Section 3, the 2013 preparatory study for the Next Generation Gravity Mission promoted and funded by ESA (see footnote 6) concludes that the "the low-low satellite-satellite tracking (LL-SST) is in practice the only observing technique potentially capable of detecting the time variable gravity signal with the required resolution", which clearly points towards an expansion of the GRACE mission concept. In 2015 this conclusion has been reinterpreted in the sense that "the gradiometer is interesting for monitoring mass transport only with a largely better performance than GOCE, or for low-cycle (4-day) gravity field retrieval (with GOCE performance gradiometer)" (quote from paper referenced to in footnote 14). These statements seem to have spurred the interest for CAI-based gravity gradiometry, which at least in principle could achieve the hoped for "largely better" performances than GOCE.

We recall that GOCE allowed determining the geoid with an accuracy of 1 to 2 cm for a spatial resolution of ~100 km. Differential accelerations were measured on-board a single satellite with ultra-sensitive electrostatic accelerometers: all the components of the gravity gradient tensor were measured with sensitivities in the range of 10–20 mE $Hz^{-1/2}$ in the 5–100 mHz measurement bandwidth, and used to reconstruct the gravity field. Due to intrinsic limitations of its electrostatic accelerometers, the GOCE gravity gradients performed poorly in the lower frequency band, where the noise power spectral density (PSD) increases with the inverse of the frequency. To counteract the low-frequency noise impact on the gravity field recovery performance, specially-tailored decorrelation filters had to be used for whitening the GOCE gradiometer noise. Conversely, a gravity gradiometer based on a cold atom interferometer would naturally provide gravity gradients with white noise at all the frequencies relevant for gravity field recovery from space, and is expected to provide gravity gradients with a sensitivity level of the order of ~5 mE $Hz^{-1/2}$.

As explained in a previous technical report [1], a CAI gravimeter is based on (i) a sequence of three Raman pulses providing a single gravity acceleration measurement (ii) a repetition of the measurement sequence to improve statistical uncertainty. Since different measurements are averaged incoherently, the statistical improvement follows the square root of the repetition rate. A CAI gravity gradiometer measures differential acceleration using two spatially separated atomic interferometers: the gravity gradient is obtained from the simultaneous acceleration measurement of two spatially separated atomic clouds in free fall. In each interferometer, an acceleration a along the direction of the Raman laser beams introduces between the two interferometric paths a phase difference given by $\Phi = kaT^2$, where $\hbar k$ is the momentum imparted by the Raman transitions onto the atoms and T is the free evolution time between two consecutive Raman pulses, also known as interrogation time. A differential acceleration measurements with two such interferometers separated by a distance D (instrument baseline) allows extracting the gravity gradient γ from the differential phase shift $\Delta\Phi = \Phi_2 - \Phi_1 = k(a_2 - a_1)T^2 = k\gamma DT^2$, where a_1 and a_2 are the accelerations experienced by the atomic clouds in the two interferometers.

The use of the same atom optics tool to manipulate the atomic wave-packet of the two clouds ensures that effects which are common to both clouds cancel out in the differential acceleration; in other terms a gravity gradiometer enables a high rejection ratio of the common mode noise sources (e.g. the vibrations of the mirror). The sensitivity of current ground-based CAI gravity gradiometers reaches a few tens of E $Hz^{-1/2}$, one major limitation being the limited interrogation time due to the free fall of atoms in a 1-g environment. An improvement of several orders of magnitude is expected in a microgravity environment, since the sensitivity scales as the square of the interaction time. An additional improvement can follow from replacing the Raman splitters with sequences of light pulses which impart multiple photon recoils, thus increasing the separation between atomic trajectories in the interferometer.

It must be pointed out that an increase in the interrogation time has an immediate impact on the instrument repetition rate, and therefore degrades the statistical uncertainty if the total time dedicated to each gravity measurement is to be left unaltered. It can be calculated that a typical interferometer phase noise at the mrad/shot level implies a sensitivity to the gravity gradient in the mE/shot range, for an interrogation time of 5 s and an instrument baseline of 0.5 m. To take advantage of such a high single-shot sensitivity a high measurement rate is necessary, which can be achieved by interrogating several atomic clouds at the same time, i.e. by using an interleaved scheme. Such an approach requires producing cold atom clouds with a cycle time significantly shorter than the interferometer interrogation time. A production time of ~1 s would yield a sensitivity in the low mE $Hz^{-1/2}$. In addition to high sensitivity, such an atom gradiometer would offer excellent long term stability. This last feature follows from its well defined and stable scale factor, which is determined by the precision with which the frequency of the laser employed to split the atomic wavefunction can be controlled. Absolute accurate measurements, with no calibration need, can therefore be realized. The absence of uncontrolled drifts would also result in an instrument noise characterized by a flat amplitude spectral density at low frequencies (i.e. below 1 mHz), in contrast with electrostatic accelerometers which feature a fast increase in the measurement noise below 10 mHz.

We now review some of the proposals which have been advanced along this line, to provide a technology assessment of satellite-based CAI gravity gradiometers and their expected performance in a simulated mission scenario.

5.3.1 Carraz 2014: a spaceborne CAI gravity gradiometer

Building on a 2012 paper[23], staff from the ESA-ESTEC stated in 2015 that "future Earth gravity missions will require gradiometers with sensitivity in the order of 1mE $Hz^{-1/2}$ over a wide spectral range", and forecasted that "atom interferometers with a baseline in the range of 1 meter are expected to meet this requirement and can be used for the realization of next-generation gravity gradiometer payloads" [24]. They therefore propose a gravity gradiometer concept which in one dimension is schematized as shown in Fig. 26. By using two MOT and two BEC cooling stages, it generates two counter-propagating atomic clouds to measure one diagonal element of the gravity tensor (V_{zz}), and the rotation rate along the x-axis. In order to obtain the full diagonal elements of the gravity gradient tensor and the full angular rate vector the scheme must be replicated to the other two dimensions.

High recoil laser pulses are used to split each cloud of atom in two and to transport the four clouds to the interferometer rooms along the z-axis, which defines the gradient axis. A second high recoil pulse brings them back to a parallel launch. Cold atoms can be prepared during the interferometric sequence to reduce the cycling time below the time of the interferometer measurement. It is thus possible to have a quasi-continuous measurement by launching atoms at a high frequency, limited by the time T_{cycle} necessary to produce cold atoms: in other terms, the interferometer will operate in an interleaved way. Best experimental results published in the literature report of a BEC of 10^4 atoms loaded in 1 s, and it can be expected in the not-too-far future to have a BEC of a few 10^6 atoms loaded in T_{cycle} = 1 s. A Bose Einstein Condensate (BEC) is required for an interrogation time of T= 5 s; in addition, to avoid loss of contrast due to the initial velocity distribution of the atom source, a point source interferometry (PSI) scheme must be used to detect the differential acceleration of 2 clouds of atoms. The authors acknowledge that, due to force gradient, the interferometer is not perfectly closed: in

[23] "The Future of the Satellite Gravimetry after the GOCE Mission", P. Silvestrin et al., International Association of Geodesy Symposia, Vol. 136, 223-230, 2012; https://link.springer.com/chapter/10.1007%2F978-3-642-20338-1_27

[24] "A spaceborne gravity gradiometer concept based on cold atom interferometers for measuring Earth's gravity field", O. Carraz et al, Microgravity Science and Technology, Vol. 26, 2014; https://link.springer.com/article/10.1007/s12217-014-9385-x

other terms, the atomic clouds at the output are not completely superimposed, which reduces the signal visibility. However, they do not study in detail this effect.

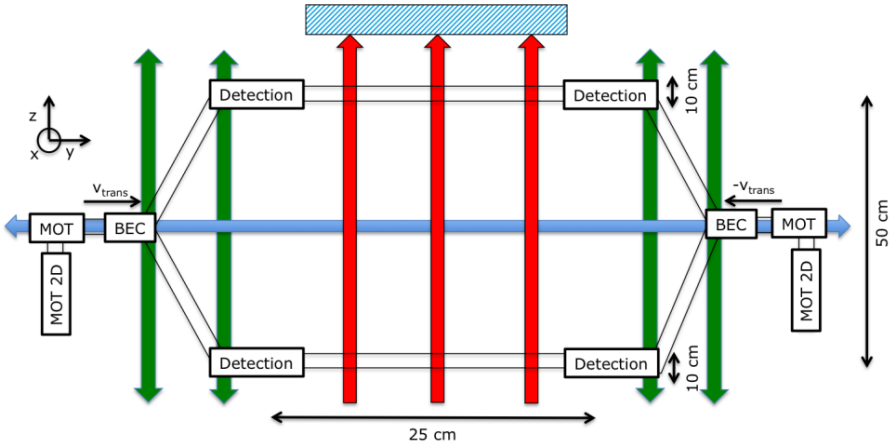

Fig. 26: One dimensional gravity gradiometer: the red arrows represent the Raman beams, the blue arrows the light pulse giving the transverse velocity, and the green arrows the light pulses guiding the atoms from the cooling chamber to the interferometer chamber. The blue rectangle is the mirror, representing the inertial reference. By carefully implementing a simultaneous detection in the 4 outputs of the interferometers, a differential signal is obtain which guarantees a high level of suppression in common noise sources, such as mirror vibration.

By using a BEC 0.4n°K with an interrogation time of 5s, a sensitivity of ~3.5 mE $Hz^{-1/2}$ is predicted, with a flat noise power spectral density at low frequencies, see Fig. 27.

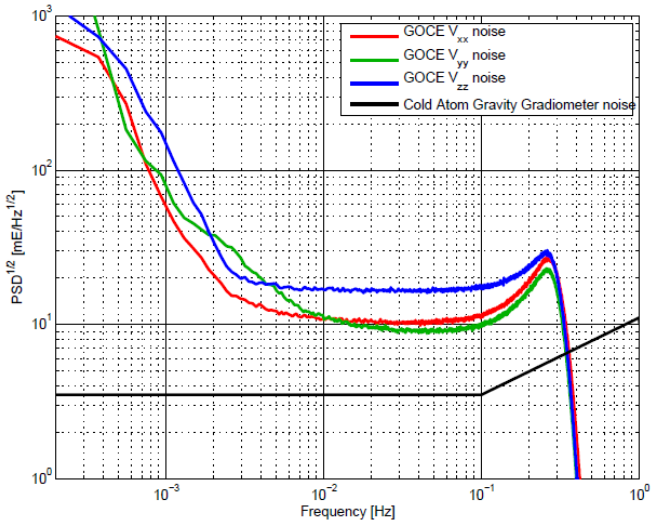

Fig. 27: Simulated noise level of the CAI gravity gradiometer (black line), as compared with GOCE's performances. Note that the CAI-based instrument noise does not increase at low frequencies. PSD: power spectral density. $PSD^{1/2}$: amplitude spectral density. In the figure, $PSD^{1/2}$=3.5 mE $Hz^{-1/2}$.

The authors acknowledge that the instrument would not be sensitive enough to provide sufficient signal-to-noise ratio on a monthly basis, so that only the static field would be recoverable. They add that "Estimation of the Earth gravity field model from the new gravity gradiometer concept has to be evaluated taking into account different system parameters such as attitude control, altitude of the satellite, time duration of the mission, etc.", and suggest that "hybridization between quantum and classical techniques could be an option to improve the performance of accelerometers on next generation gravity missions", to correct the spectrally colored noise of the electrostatic accelerometers in the lower frequencies, as already explained in Section 5.1.

5.3.2 Douch 2018: field recovery performances

Following the design proposed by Carraz 2014 (see previous subsection), a group composed by researchers from Leibniz University (Hannover) and LNE-SYRTE (Paris) simulated the performances of the CAI gravity gradiometer in an actual mission scenario[25]. The authors note that although the various proposals for future space gravity missions emphasize the need to sustain a continuous monitoring of the time-variable gravity field, a CAI gradiometer like the one proposed by Carraz is not sensitive enough to detect the corresponding signals with a sufficient signal-to-noise ratio on a monthly basis. Indeed, starting from the monthly time-variable gravitational signal computed from the ESA Earth System Model (which contains the contribution of the atmosphere, oceans, cryosphere, land hydrology and solid Earth), they demonstrate that to detect the time variable gravity gradient components V_{xx}, V_{yy}, and V_{zz} with an SNR larger than 1, an instrument with a sensitivity better than 0.1 mE $Hz^{-1/2}$ is required: conversely, the CAI gravity gradiometer proposed by Carraz has a sensitivity of 3.5 mE $Hz^{-1/2}$. The study is therefore focused on the ability of a CAI gradiometer mission to recover the static gravity field: the GOCE mission represents therefore the right benchmark to evaluate the performance of the CAI gradiometer and to quantify precisely how it can improve the knowledge of the static field.

The gradiometer configuration shown in Fig. 28 enables a measurement of the gravity gradient along the direction of l, which constitutes the gradiometer baseline. Such configuration must be replicated along the other two axes if a 3-dimensional measurement is desired.

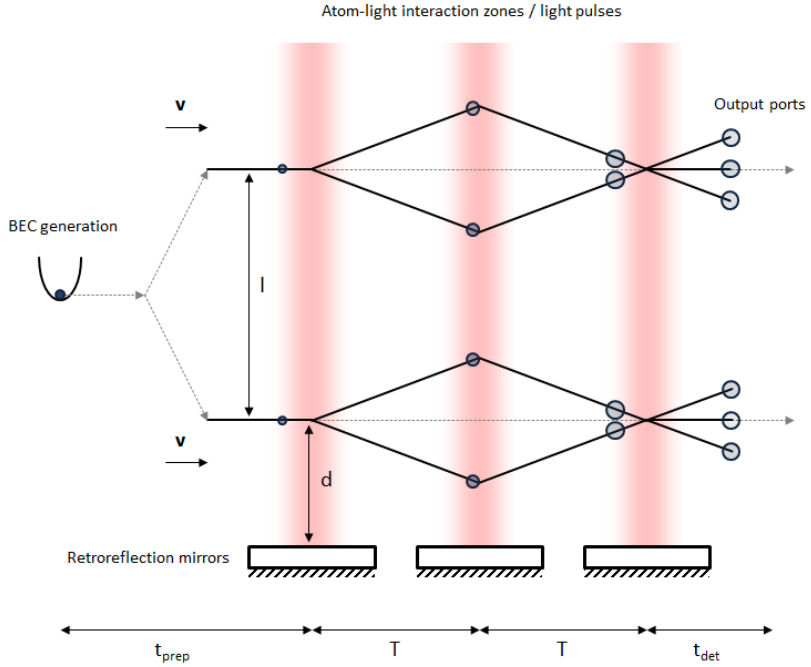

Fig. 28: Atom interferometry scheme for gradiometric measurements as proposed in Carraz et al. (2014). During the preparation time t_{prep} an atomic ensemble is generated, split into two clouds separated by l (the instrument baseline), and injected into the two atomic interferometers with forward velocity $\mathbf{v}$. With t_{prep} shorter than 2T, two or more clouds can be at different stage of the interferometric sequence (interleaving), thus increasing the measurement rate. In this representation, the atomic ensembles are in free fall, so they follow linear trajectories. The red stripes in the figure represents the interferometers laser beams, which cause in the atoms stimulated Raman transitions with an associated atomic momentum change $\hbar \boldsymbol{k}_{eff}$ in the same direction of the laser beams. The instrument has a sensitivity of 3.5 mE $Hz^{-1/2}$, which corresponds to a white noise with a one-sided amplitude spectral density (ASD) of 3.5 $\sqrt{2} \cong 5$ mE $Hz^{-1/2}$.

[25] "Simulation-based evaluation of a cold atom interferometry gradiometer concept for gravity field recovery", K. Douch et al., Advances in Space Research 61 1307–1323, 2018
https://hal.sorbonne-universite.fr/hal-01826234/document

To understand the issues analyzed in the paper, we need to introduce some preliminary concepts on the orientation of the satellite and of the on-board gradiometer. The pointing mode of an orbiting satellite is determined by the needs of its specific mission: as depicted on the left side of Fig. 29 we can have target pointing, nadir pointing, or inertial pointing. Target pointing is obviously adopted when the object of interest is located in a fixed location on the Earth surface. In inertial pointing the satellite orientation is kept constant during the orbital motion, in order to obtain in it a quasi-inertial system of reference; such a pointing is technically quite difficult, and has been used only for very specific scientific missions. Gravity observations typically use nadir pointing: the satellite is kept orientated along the vertical direction, which implies a continuous rotation during its orbital motion. On the right side of Fig. 29 we introduce the three axes x, y, and z which determine respectively the along-track, cross-track and nadir directions determined by the orbital plane.

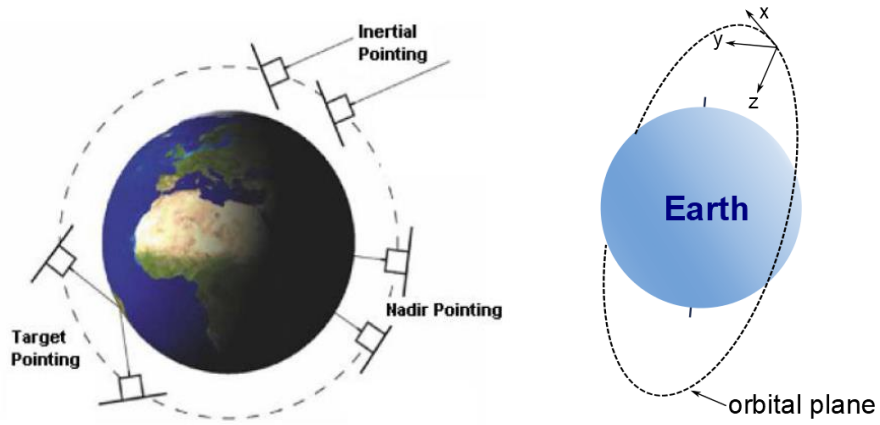

Fig. 29: Left: different possible pointing options of a satellite. Right: representation of the axis indicating the along track (x), cross-track (y), and nadir (z) directions.

A typical GOCE-like orbit would imply a rotation rate of $\Omega \sim 1$ mrad/s affecting the interferometers oriented in the along-track and in the nadir directions. This rotation prevents the atomic trajectories from closing at the third interferometric pulse: indeed, it can be calculated that the separation between the clouds of atoms which have followed the upper and the lower path in each one of the two interferometers is larger than the dimension of the atomic clouds themselves. The fringe contrast therefore diminishes to the point that no output signal is recorded by the interferometer: it has been calculated that a reduction of the rotation rate by a factor of ~1000 is required to recover the contrast.

Let us also recall (see e.g. [1]) that the interferometric phase shift is determined by two contributions, respectively associated to linear acceleration and to rotation

$$\Delta\Phi = \Phi_{\boldsymbol{a}} + \Phi_{\boldsymbol{\Omega}} = \boldsymbol{k}_{\mathrm{eff}} \cdot \boldsymbol{a}\, T^2 + 2\boldsymbol{k}_{\mathrm{eff}} \cdot (\boldsymbol{\Omega} \times \boldsymbol{v})\, T^2$$

A rotation-induced phase shift $\Phi_{\boldsymbol{\Omega}}$ therefore appears whenever a drift velocity $\boldsymbol{v}$ is present. In the original Carraz proposal, the atoms are launched into the interferometer with a forward drift velocity $\boldsymbol{v}$ ~2.4cm/s. This shift is cancelled in the differential signal between the accelerometers which contains the information of the gradient, but only if the forward drift velocities are the same for both. Due to the velocity spread and the finite number of atoms per ensemble, a random velocity uncertainty which is uncorrelated between the interferometers will remain. This limits the maximum rotation rate compatible with shot-noise-limited performances to ~1 μrad/s, a value similar to the requirement for closing the interferometer.

It is also to be observed that the velocity distribution in each atomic cloud implies a velocity-dependent dephasing, so that the signal over any output port becomes spatially fringe-patterned if the rotation rate significantly exceeds ~ 1 μrad/s: as a consequence, the signal given by the atom population count at the port vanishes. An antidote could be

a mirror counter-rotation which cancels the satellite rotation rate, but the interleaved operation mode and the dynamic range requirements prevent pursuing this option. It is finally to be noted that also a gravity gradient parallel to $\boldsymbol{k}_{\mathrm{eff}}$ leads to a non-closed atom interferometer, with a displacement at the last beam splitter pulse parallel to $\boldsymbol{k}_{\mathrm{eff}}$.

Summarizing, the component of the angular velocity perpendicular to the measurement axis must be smaller than 1μrad/s: as a consequence, only nadir pointing and quasi-inertial pointing modes are possible. If the nadir pointing mode is chosen, a maximum rotation rate of ~1 μrad/s can only be maintained in the cross-track y direction. If quasi-inertial pointing mode is chosen, a maximum spurious rotation rate of 1 μrad/s along all three axes must be ensured. With nadir pointing a 1-axis instrument is to be adopted, since only the V_{yy} component of the Gravity Gradient Tensor can be measured; in this configuration, the laser beams and the instrument baseline l are directed in the cross-track y direction, and the y component of the acceleration is measured at the two interferometers to produce the differential signal. With quasi-inertial pointing a 3-axis instrument could produce all the diagonal components V_{xx}, V_{yy} and V_{zz} of the gravity gradient tensor.

An 8-months mission is simulated for an altitude orbit of 239 km. In addition to the orbit and its precision (2.6cm, as in GOCE), other input parameters include the noise of the star tracker, the noise of the gyroscopes, and the gravity gradiometer noise, which is taken to be 5 mE $Hz^{-1/2}$. The results of the gravity field recovery performance are shown in Fig.30 in terms of geoid height degree variance. The GOCE solution error is obtained by computing a gravity model based on the three diagonal gravitational gradients of the whole GOCE mission period (November 2009 – October 2013, about 47 months), and it is compared to two different reference gravity models, namely EIGEN-6C4 and GOCO05S.

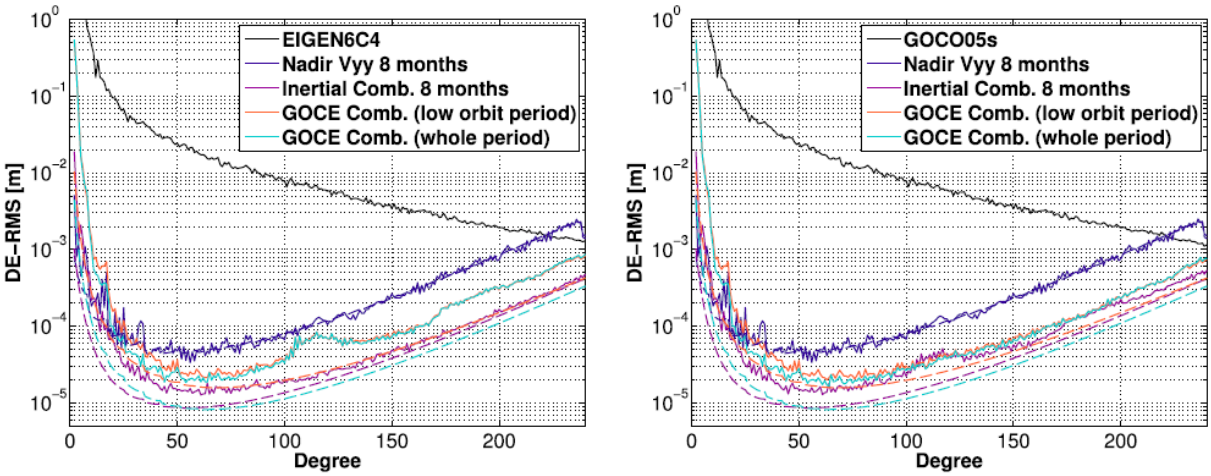

Fig. 30: Gravity field recovery performance for the CAI gravity gradiometer and for GOCE. EIGEN-6C4 and GOCO05S indicate two well-established reference gravity models. "Comb" means the GGT solution in which the three gravity gradients are combined to produce a single synthetic indicator. Solid curves represent the true errors (i.e. the differences between the recovered gravity field coefficients and the input background model) and dashed curves are formal errors (i.e. the accompanied standard deviations of the parameters). The gradiometer nominal noise is 5 mE $Hz^{-1/2}$. It can be noted that the black curves corresponding to EIGEN-6C4 and GOCO05S are identical, so we can suspect a mistake here. A curve for EIGEN-6C4 is given also in Fig. 35.

The nadir mode does not allow outperforming GOCE under identical orbit and measurement timespan, while the solution in the quasi-inertial mode is significantly better than the nadir mode one, especially above the spherical harmonic degree ~50. As a consequence, the nadir mode should be discarded in favor of the quasi-inertial mode. The 8-month quasi-inertial solution is better than the GOCE solution for the whole mission period. An 8-month mission at an altitude of 239 km and using a 3-axis CAI gradiometer with a nominal white noise of 5 mE $Hz^{-1/2}$ in the quasi-inertial mode would outperform the full GOCE mission and eventually yields a more precision gravity field model. Nonetheless, it should be borne in mind in this comparison that the GOCE satellite

was most of its lifetime at a higher altitude than 239 km; for a fairer comparison, the GOCE solution is also plotted, for the 8 months during which the satellite was at an altitude equal or lower than 239 km. Again, the 8-month quasi-inertial solution at a constant altitude yields a slightly better solution despite the fact that the 8-month GOCE solution is partly based on gravity gradients measured at a lower altitude.

The authors acknowledge that, among the various assumptions made in their study, the attitude control requirements and the quasi-inertial mode are particularly challenging, especially at such a low altitude where the atmospheric drag may cause variations on the satellite angular velocity greater than 1 μrad/s. Indeed, inertial pointing satellites are rather uncommon although control feedback strategies to maintain such pointing have been studied. We conclude by quoting verbatim their main conclusions:

"Our simulations show that the nadir mode does not allow to clearly outperform GOCE. The results are more promising in the case of the quasi-inertial mode where the gradiometer can measure the three diagonal components of the GGT. To outperform the whole GOCE mission in term of geoid accuracy, we conclude that a 3-axis CAI gradiometer with a nominal white noise of 5mE/√Hz is required, at an altitude of 240 km, in quasi-inertial mode, for at least 8 months. […] Although the quasi-inertial mode proved to be the best operating mode for the CAI gradiometer considered in this study, keeping such a pointing seems technically challenging. Therefore we recommend to investigate whether it is possible to modify the design of the CAI gradiometer so that the 3 diagonal elements of the GGT can be measured in the nadir mode. In other words, an improved interferometer architecture that allows the atoms to interfere in an almost uniform rotation reference frame is highly desirable."

5.3.3 Trimeche 2019: concept study and preliminary design

The outcome of the previous study led its authors to collaborate with researchers from LP2N (Bordeaux), ZARM and DLR (Bremen), ISMO CNRS (Orsay), to investigate how to fly the gradiometer in the nadir mode by correcting its angular rotation[26]. They propose a compensation of all the angular rotations in the nadir pointing mode by tilting the three interferometric mirrors, both statically and dynamically. To our knowledge, this is the most complete study of a CAI gravity gradiometer published until now: only the most significant conclusions of its detailed technical analysis are reported here. The overall scheme of the instrument and some details of its components are shown in Fig. 31.

The interferometer is linked to the satellite frame, which orbits at a fixed altitude with a constant orbiting frequency Ω_{orb}. The measurement axis, which is the one along which the laser beams propagate, is taken in the orbital plane; the rotation rates of the satellite along the along-track (x), cross-track (y), and nadir (z) directions are Ω_x, Ω_y, and Ω_z, as shown in Fig. 29. In the case of nadir pointing, $\Omega_y = \Omega_{orb}$ and $\Omega_x \approx \Omega_z \approx 0$, while for inertial pointing $\Omega_x \approx \Omega_y \approx \Omega_z \approx 0$. For an altitude of 250 km, $\Omega_{orb} = 1.2$ mrad s^{-1}.

The rotation of the satellite must be compensated in order to obtain mirrors with a fixed orientation in the frame of the atoms. This can be obtained by tilting the first and the last retro-reflecting mirrors of the interferometric sequence by angles $\pm\theta = \pm\Omega_y T$, where Ω_y is the rotation rate along the cross-track axis y and T is the time separation between two successive interferometric pulses, see Fig. 32. This configuration removes the sensitivity of the interferometer to centrifugal and Coriolis accelerations. The phase shift induced by the gravity gradient must also be compensated, which can be done by changing the Raman wavevector of the second pulse by an adequate amount δk.

[26] "Concept study and preliminary design of a cold atom interferometer for space gravity gradiometry", A. Trimeche et al., Class. Quantum Grav. **36,** 215004, 2019
https://iopscience.iop.org/article/10.1088/1361-6382/ab4548

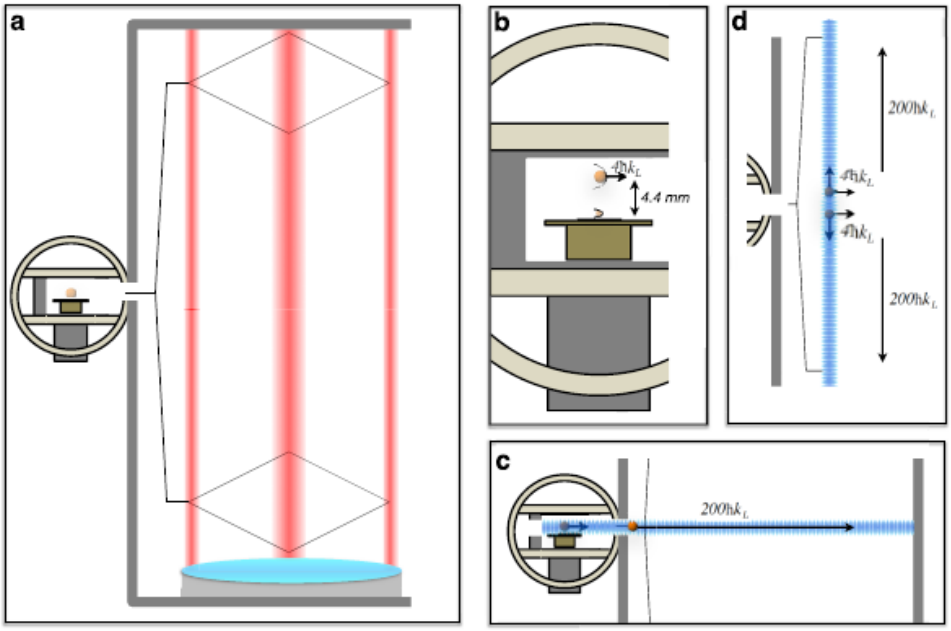

Fig. 31:(a) Global scheme of the gravity gradiometer, which relies on the double diffraction interferometric technique (b) The BEC source, based on an optimized atomic chip design, generates ~10^6 atoms which are then magnetically evaporated, displaced and collimated to form clouds at ~100p°K (c) Horizontal transport to the interferometry chamber (d) The BEC is split in two by the combination of a double Raman diffraction and a twin-lattice technique feeding both interferometers. In total, the entire process of production, manipulation and transport of the BEC takes 1.4 s. A new magneto-optical trap (MOT) production can start as soon as the previous produced BEC has been loaded into the vertical lattices resulting in an effective cycle time of only 1.2 s, which combined with an interrogation time of 10 s allows interleaving up to 8 measurements.

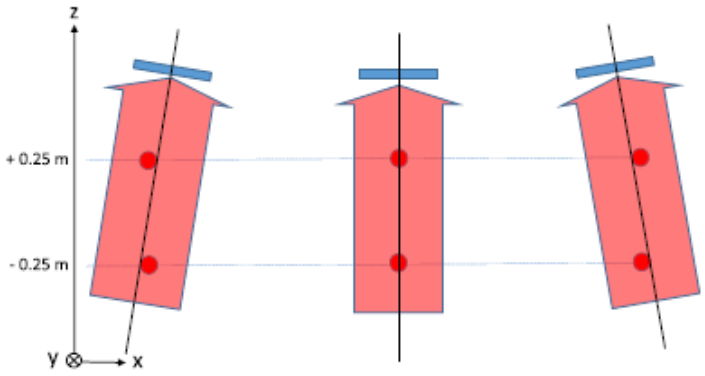

Fig. 32: Tilted mirrors in the three-pulse interferometric sequence. The relative angle between two consecutive reference mirrors is ~7 mrad, corresponding to the mean rotation rate of the satellite. The first and the third mirror in the Figure are for the $\pi/2$ pulses: such mirrors are fixed on piezoelectric tip-tilt mounts to allow the fine control of the relative angle between the three reference mirrors. A dynamic range of ±30 μrad and an accuracy of 10 nrad is needed, specs which which according to the authors are "slightly beyond" the technological state-of-the-art.

The general architecture of the system to be employed to measure the gravity gradient tensor components T_{zz} and T_{xx} is represented in Fig. 33. For each 1-D instrument, four mirrors are fixed inside the vacuum system: one for the two vertical Bloch lattices and three tilted reference mirrors for the interferometer, which compensate the satellite rotation and its associated bias and contrast loss. The 1-D interferometer to be used for the T_{yy} component needs a single reference mirror for the splitting and the interferometer pulses, and no tip-tilt mount is necessary.

A careful error budgeting analysis is performed, whose details are outside the scope of the present Report. We report verbatim one of its main conclusions: "while the requirements on the control and knowledge of Ω_x and Ω_z can be met with current

technologies, using for instance fiber optic gyroscopes of the Astrix class, the ones of the rotation rate Ω_y, and of the mismatch of the mirror with respect to the ideal tilt, are very stringent, and cannot presently be met, even with the best space qualified gyroscopes. Instead we propose to use the mathematical properties of the gravity tensor, and its null trace, to estimate Ω_y, or at least its fluctuations."

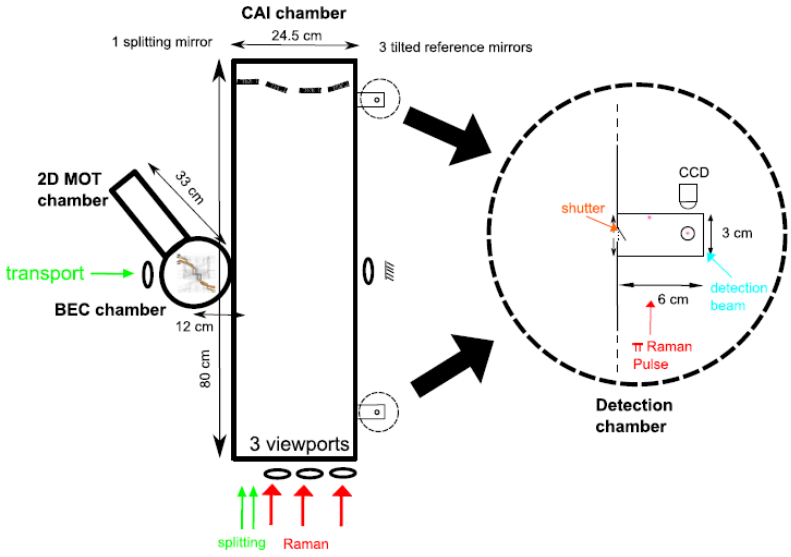

Fig. 33: Architecture of the 1-D instrument to be used for T_{zz} and T_{xx}. An atom beam is produced in the 2D MOT chamber and used to load a mirror 3D MOT on a chip in the BEC chamber, where the ultra-cold atom source is achieved. The atom cloud is then launched thanks to a Raman pulse and horizontal Bloch lattices towards the CAI chamber where the differential interferometer is produced. The atom cloud is slowed down thanks to horizontal Bloch lattices, then split and transported at the entrance of the interferometer area by applying vertical Bloch lattices. The detection is achieved in a separated small chamber in order to avoid parasitic light in the CAI interferometric chamber.

Fluorescence detection is employed for atomic counting at each of the interferometers output; CCD cameras are used to obtain spatial resolution, which is necessary to prevent the contrast loss determined by the inhomogeneous dephasing due to initial velocity and position distribution. It also allows the extraction of information on velocity dependent phase shifts. In Fig. 34 it is shown how the count spatial distribution at an output port depend on Ω_y. It can be seen that a suboptimal compensation of the rotation destroys the output signal.

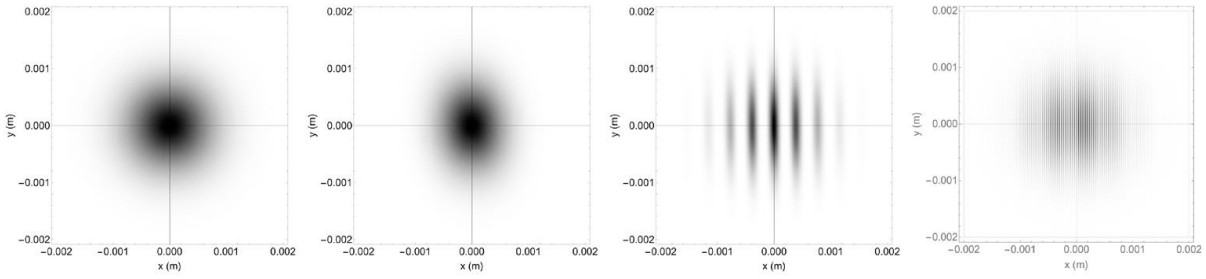

Fig. 34: Simulation of interferometer fringes expected to be obtained for a point-source atomic cloud in the x–y plane for different values of Ω_y. From left to the right: 1×10^{-6} rad s^{-1}, 1×10^{-5} rad s^{-1}, 1×10^{-4} rad s^{-1}, and 1.17×10^{-3} rad $s^{-1} = \Omega_{orb}$.

The paper provides a design of the instrument and its main subsystems, including the laser sources (based on telecom technologies and second harmonic generation), the mirrors, the magnetic field and the magnetic shields. The main characteristics of the instrument are summarized below, and the glossary in Section 6 provides a brief explanation of the technical terms:

- BEC of ~10^6 atoms generated from an atomic chip
- Further cooling to T < 100p°K via magnetic evaporation
- BEC splitting by combination of double Raman transitions and twin Bloch lattice
- Interrogation time 2T=10s, cycle time: T_c=1.2s, 8 interleaved measures;
- Delta-kick atomic cloud collimation
- Horizontal and vertical Bloch optical lattices for atomic transport
- Nadir pointing enabled by static & dynamic tilting mirrors
- Pointing errors <1 mrad
- Attitude control Ω_x, $\Omega_y - \Omega_{orb}$, $\Omega_z < 10^{-6}$ rad s^{-1}
- Mirror tilt stability < 5 nrad
- Spatially resolved detection
- Sensitivity: 3.5 mE at 1 s
- Noise: 5 mE/$Hz^{1/2}$
- 239km height orbit, 8 months mission
- Three axis instrument: 800kg, 3000W, 1x1x1.6m

A performance analysis via a closed-loop simulator which allows to precisely quantify the errors in the gravity field solutions is also included, assuming that the instrument with a nominal white noise of 5 mE $Hz^{-1/2}$ will be used in an 8-month mission at an altitude of 239 km. As shown in Fig. 35 (to be compared with Fig. 30 of the previous subsection), the CAI solution for the three-axis nadir pointing mode would perform better than the GOCE solution for the whole mission period.

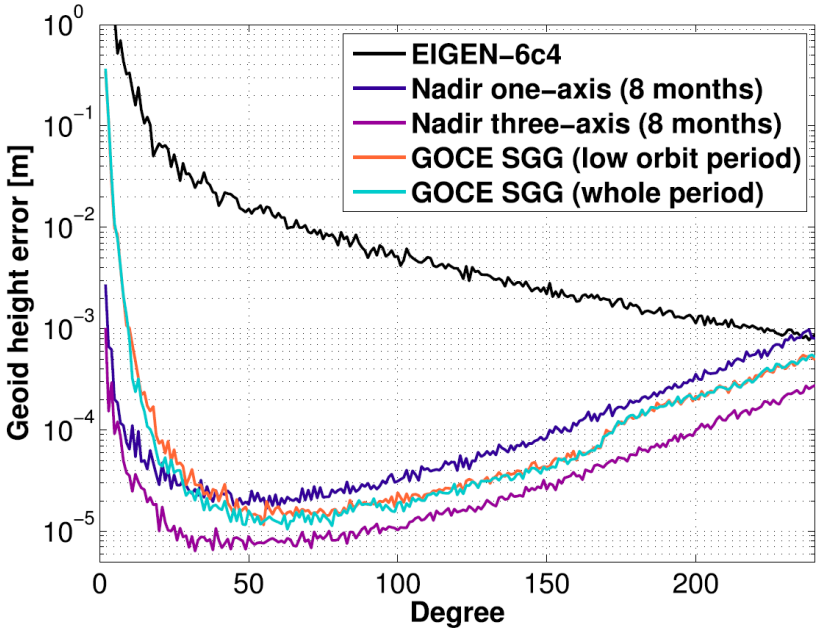

Fig. 35: Geoid height error for the nadir-pointing gravity gradiometer, assuming an 8-month mission at an altitude of 239 km and using an instrument with a nominal white noise of 5 mE $Hz^{-1/2}$. It is evident that a 1-axis instrument would not outperform the GOCE satellite gravity gradiometer (SGG). Conversely, the CAI gradiometer in the three-axis nadir mode at a constant altitude yields a better solution than GOCE, despite the fact that the 8 month GOCE solution is partly based on gravity gradients measured at a lower altitude.

The development of such an instrument represents a non-minor technological challenge, as the authors themselves acknowledge: "The determination of the optimal gain requires a realistic mission scenario, which remains to be investigated. As inputs, such mission-oriented study would use the constraints which we have determined for the attitude control and the overall size, weight and power (SWaP) budget of the total instrument. This budget has been established considering existing and available technology, and certainly needs to be reduced to end up with a more reasonable load. Possible modifications to the design, such as sharing subsystems between the instruments, would certainly help, but it is clear that a number of specific technological and engineering efforts are also required, in particular directed towards the optimization of the power consumption. This challenging task motivates on-going and future research and development activities. This concerns not only the technological efforts mentioned above, to improve for instance the generation of BEC sources on atom chips or the compactness and power consumption of fiber-based laser systems, but also the validation of the instrument concept. Indeed, if the key scientific methods, such as Bloch-lattice transport, double Raman diffraction or interleaved measurements, have for most of them been demonstrated individually, demonstration activities combining several, and in the end all, of them in a single setup in a representative environment, need to be pushed. This calls for carrying prototyping activities, such as developing an elegant breadboard model of the sensor and characterizing it in a relevant environment. A thorough assessment of the performances of such a prototype will establish gradiometers based on cold atom interferometry as appealing sensors for future gravity missions aiming at improving our knowledge of the Earth's gravity field."

5.3.4 Migliaccio 2019: satellite mission concept

This study[27] analyses a CAI gravity gradiometer to conclude that an improvement with respect to GOCE could be obtained in the estimate of the static gravity field over all the harmonic spectrum, and that results are promising also for the time-variable gravity field, although GRACE would still be performing better at very low degrees. The paper also simulates geophysical phenomena such as mass changes due to hydrology, glaciers and tectonic effects: by taking into account the expected gravity change-rates, time constants and spatial frequencies, it shows that signals invisible to past satellites could now be detected. This study is less focused on the CAI gradiometer technological aspects than on its performances in a whole simulation mission, thus taking into account the point of view of the actual users of the mission data.

An inter-pulse separation T = 5 s and a repetition rate of 1 Hz as in Carraz 2014 is assumed. The authors acknowledge that operating an atom interferometer in a rotating frame requires a counter-rotation in the Raman wave-vector to compensate for the Coriolis acceleration, which is not compatible with the use of counter-propagating atom clouds, as originally proposed by Carraz to implement rotation rate measurements. A simplified setup (see Fig. 36) with a single pair of atom clouds propagating in the same direction is therefore considered. A passive, static counter-rotation of the laser wave-vector is used to compensate the average value of the satellite rotation rate, implementing the angular dynamic range ($\Omega_{orb}T \approx 7$ mrad) required for rotation compensation. The authors assume that small residual rotation errors can be compensated by active tip-tilt actuation on the last retro-reflection mirror, without giving any demonstration of its technological feasibility.

To ensure a high enough S/N ratio atom clouds at nanokelvin temperatures are required. Their generation involves using a high-flux atomic source such as a 2D-MOT, which loads a three-dimensional magneto-optical trap (3D-MOT) where trapping and cooling to microkelvin temperatures is performed. The atoms are further cooled to form a Bose–Einstein condensate (BEC) at nanokelvin temperature using delta-kick cooling. Such

[27] "MOCASS: A Satellite Mission Concept Using Cold Atom Interferometry for Measuring the Earth Gravity Field", F. Migliaccio et al., Surveys in Geophysics, 40, 2019
https://link.springer.com/article/10.1007/s10712-019-09566-4

ultra-cold atoms are then sent to the main vacuum chamber with a velocity of ~25 mm/s using an optical lattice to impart several photon recoils in a direction orthogonal to the gradiometer sensitive axis. In the main chamber, the atoms are illuminated with a sequence of two optical lattice pulses along the gradiometer sensitive axis, to split the atoms into two clouds with a separation of $d \approx 50$ cm. The two atomic clouds are simultaneously illuminated with Raman light pulses to implement the interferometric sequence and are finally detected with fluorescence imaging.

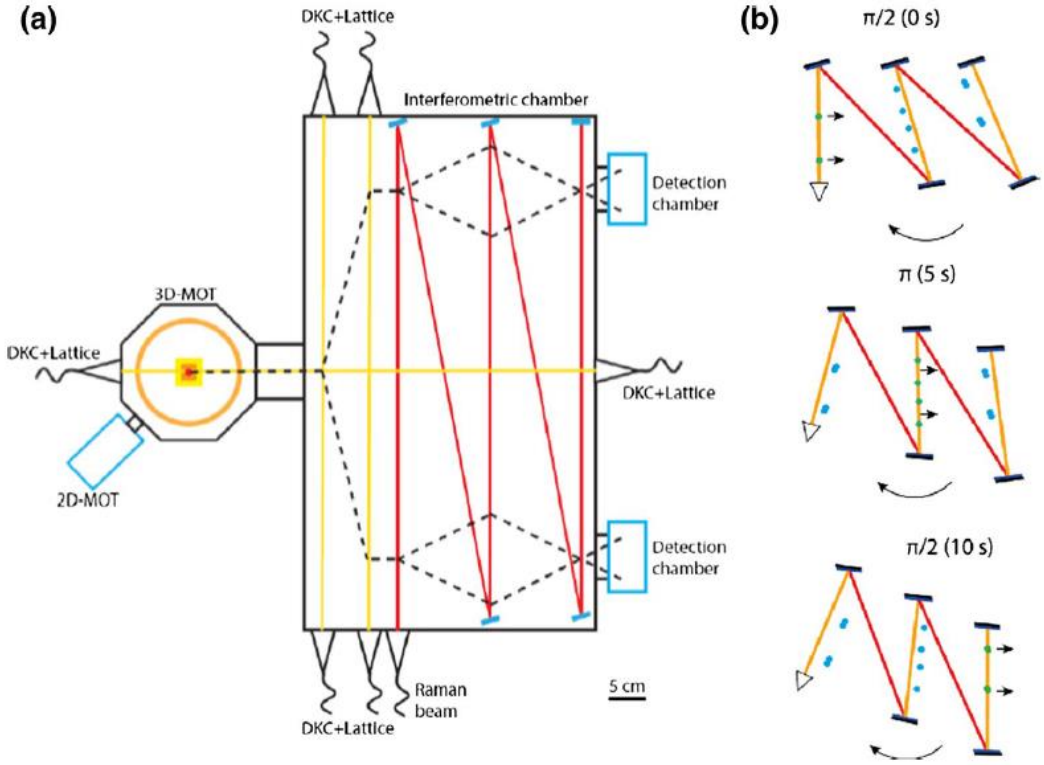

Fig. 36: (a) The CAI space gradiometer payload: solid black lines indicate the mechanical structure of the vacuum chamber; dashed black lines indicate the trajectories of atom clouds; yellow lines indicate laser beams for delta-kick cooling (DKC) and optical lattices providing precise momentum kicks to the atoms; red lines indicate Raman laser beams for the atom interferometry splitters. (b) Static compensation for spacecraft rotation in order to cancel Coriolis acceleration: mirrors are aligned to form an angle $\Omega_{orb}T$ between the Raman wave-vectors at successive pulses.

A radial cold atom gradiometer is considered, meaning that the sensitive axis (determined by the direction of the Raman wave-vector as well as by the separation of the two atomic clouds) is approximately along z, and the launch velocity of the atom clouds is along the x-axis. If the Raman beam is counter-rotated at an angular rate $\sim -\boldsymbol{\Omega}$, the atom interferometer phase depends on the residual rotation rate $\delta\boldsymbol{\Omega}$ of the optical wavevector. For simplicity, the only non-vanishing component of the residual rotation is assumed to be $\delta\Omega_y$, i.e. the one along y only, which gives the major contribution. Under these assumptions, the gradiometer phase turns out to be

$$\Phi = 2k_{eff}T^2T_{zz}d + k_{eff}T^2T_{zz}(\delta z + \delta v_z T) + 2k_{eff}T^2 d\delta\Omega_y^2 + 4k_{eff}T^2\delta v_x\delta\Omega_y^2$$

Here d is the interferometer baseline, T_{zz} the diagonal component in the z-direction of the gravity gradient tensor, while δz and δv_i indicate errors on the differential position and velocity of the two atom clouds. The first term represents the gradiometer readout signal, the following terms are the main error contributions due to local gradient, centrifugal acceleration and Coriolis acceleration. In particular, the second and fourth phase terms depend on the coupling of gravity gradient and angular velocity components respectively with the components of atomic differential positions and velocities. Such

terms produce both errors in the gradient measurement, due to non-vanishing mean values of the differential position and/or velocities of the atomic clouds, and a loss of contrast in the atom interferometer due to the finite temperature of the atoms. The centrifugal acceleration term produces errors in the gradient measurement. The Coriolis and centrifugal terms can be largely mitigated with counter-rotation of the Raman wave-vector across the interferometric sequence, while the noise term due to local gradient can be efficiently mitigated with a suitable chirp of the Raman laser frequency during the interferometric sequence.

The amplitude spectral density (ASD) of the gravity gradient noise for the CAI interferometer is shown in Fig. 37, which is to be compared with the one reported in Fig. 27 for GOCE and for the Carraz 2014 proposal.

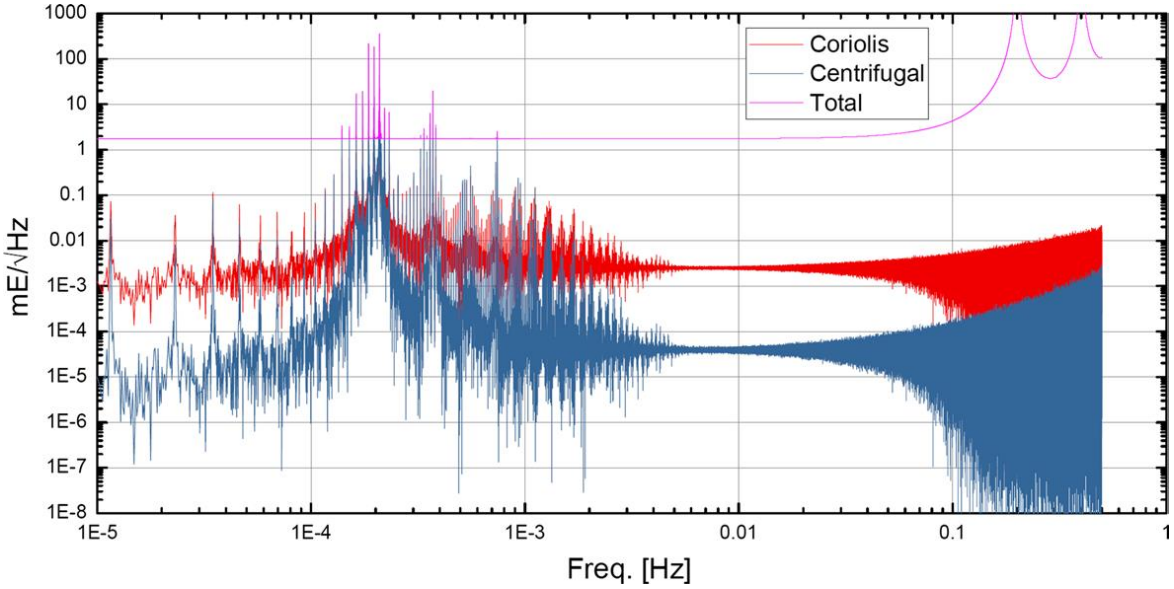

Fig. 37: Total amplitude spectral density of the gravity gradient noise with its dominant components, in the nadir-pointing mode and radial (z) sensitive axis. Main assumption for the simulations are fluctuations of 10 μm/s RMS for the residual velocity difference between atom clouds, a typical GOCE-like orbit, and a compensation of the rotation rate at the level of 10^{-8} rad/s.

To explore and quantify the advantages that MOCASS could provide with respect to previous gravity missions, several simulations have been carried out and the data have been analyzed. The technical details of the simulation procedures are outside the scope of the present Report, and we just mention that two different cold atom interferometer configurations have been considered: (1) a single-arm gradiometer, which measures the gradient of the potential in one direction (T_{xx}, T_{yy}, or T_{zz}) and (2) a double-arm gradiometer, which measures T_{zz} and T_{xx}, or T_{zz} and T_{yy}.

For the payload, the outcome from the computations of the cold atom interferometer sensitivity in the different possible configurations has been used in the form of error PSD. For the orbit data, the parameters of the GOCE orbit have been applied regarding altitude and inclination of the mission, namely almost-circular Sun-synchronous orbit at two different altitudes: "high" (~ 259 km) and "low" (~ 239 km). The time span of the simulation is 2 months, and the static gravity field is sampled from the EIGEN_6C4 global model. Two possible pointing modes have been considered: the nadir-pointing mode and the inertial one. It is understood that the inertial-pointing mode at such low altitude would be extremely challenging from a space system engineering point of view. The RMS of the predicted errors are summarized in Table 6, which shows that the nadir-pointing is expected to give better performance anyway.

Pointing mode	Orbit	Error RMS of predicted T_{rr} values (mE)				
		T_{xx}	T_{yy}	T_{zz}	T_{xx} and T_{zz}	T_{yy} and T_{zz}
Nadir-pointing mode	High orbit (~259 km)	1.22	1.76	*0.36*	0.56	*0.55*
	Low orbit (~239 km)	0.92	1.29	*0.22*	0.30	*0.34*
Inertial-pointing mode	High orbit (~259 km)	4.52	*0.45*	2.91	0.76	*0.55*
	Low orbit (~239 km)	1.49	*0.33*	2.77	0.40	*0.34*

Table 6: Errors forecasted in the gravity gradient components, for single arm and double arm gradiometer in different orbit configurations.

To appreciate the impact of these numbers in the reconstruction of a global gravity model, Fig. 38 shows the error degree variances for MOCASS for a 2-month mission in high orbit with a single-arm gradiometer in the case of T_{zz} observations (nadir-pointing mode) or T_{yy} observations (inertial-pointing mode). The curves are compared with the corresponding curves for the GRACE and GOCE error degree variances and show the improved behaviour of the MOCASS results, apart from the low-frequency spherical harmonics, where GRACE results remain superior. However, MOCASS would still not provide much extra resolution of the hydrological signal.

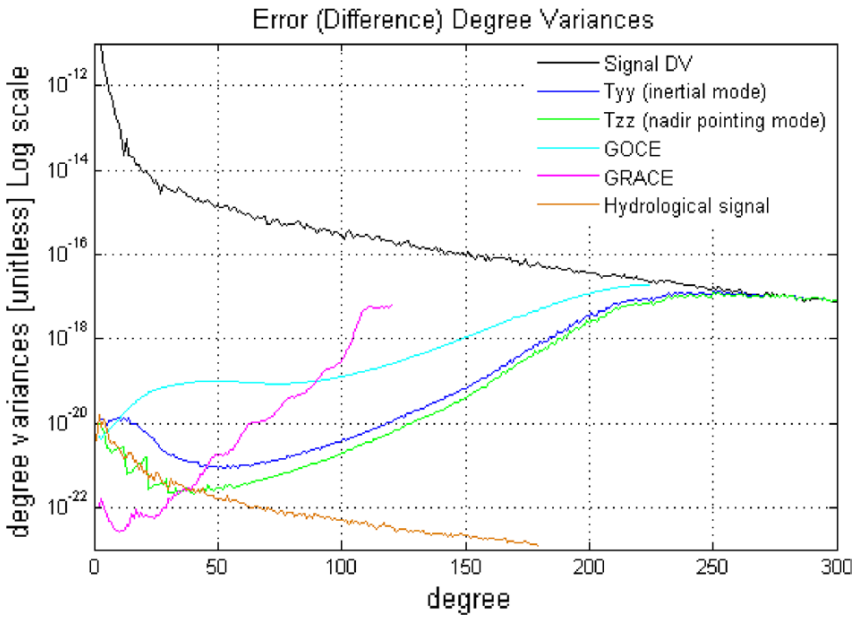

Fig. 38 Error degree variances in terms of reconstruction of a global gravity model for a 2-month MOCASS mission in high orbit and observations of a single-arm gradiometer; as a comparison, 2-month GOCE and GRACE solutions are represented, as well as the degree variances of the static gravity signal and the hydrology signal.

For a static gravity field model, the quality of the solution improves by exploiting a much longer observation period, as shown in Fig. 39 (left) which displays the gravity anomaly error Δg at ground level for mission periods of 1, 2 and 5 years. The right side of Fig. 38 shows the level of accuracy attainable by MOCASS in estimating the time-variable gravity signals, by displaying the cumulative errors in estimating a linear trend of gravity anomalies, with monthly solutions.

In the same Fig. 39 the performance of GOCE and Grace are also reported. For the static gravity field, an improvement with respect to GOCE performances is seen over all the harmonic spectrum (error of ~ 1.4 mGal at degree 300, ~ 0.9 mGal at degree 250 for a 5-year-mission). For the time-variable gravity field: the MOCASS error estimates are

promising (the 2-month solution is better than the GRACE one already above degree 40, while in the case of GOCE this occurs above degree 90). However, the accuracy at very low degrees seems to be still insufficient for this type of applications. It has to be stressed that a mission in nadir- or inertial-pointing mode at such altitude, including the required attitude control, is very challenging from the engineering point of view.

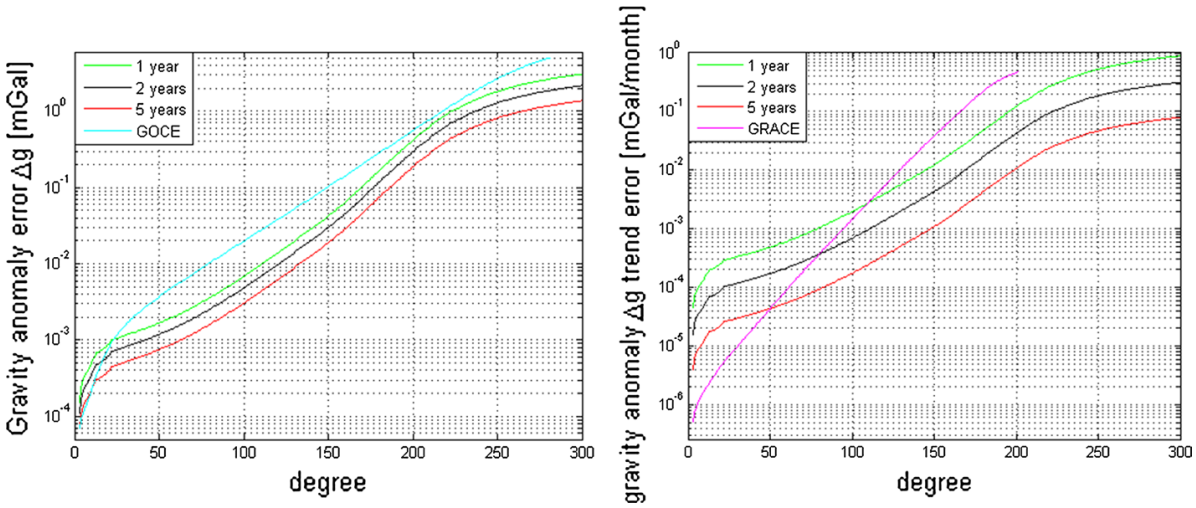

Fig. 39: Left: stationary field recovery performance of MOCASS with respect to GOCE. Right: monthly field recovery performance of MOCASS with respect to GOCE. Missions with durations of 1, 2 and 3 years are considered, using a *Tzz* instrument in high orbit nadir-pointing mode.

A significant part of the study is dedicated to the evaluation of the impact of the mission for the improvement in the detection and monitoring of geophysical phenomena, estimating the progress that could be achieved. Simulations of different phenomena were performed, including (i) deglaciation in High Mountain of Asia (HMA) (ii) mountain building processes (tectonic), (iii) continental hydrology, and (iv) volcanic eruptions leading to growing seamounts. For each of these phenomena, the increase of signal detectability with respect to GRACE or GOCE was estimated. As an example, Fig. 40 shows the progress in glacier monitoring which would be made possible by MOCASS.

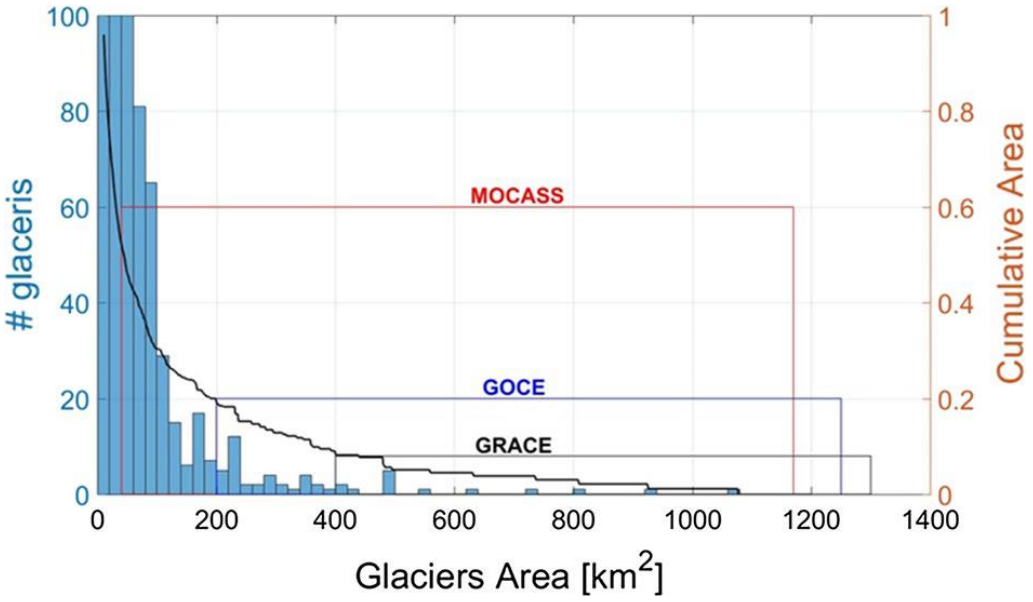

Fig. 40: An example of geophysical phenomena previously undetectable

6 Glossary

The reader is referred to our background technical report on CAI sensing [1] for a basic understanding of the physics and the technologies which are commonly employed to leverage cold atoms properties. Here we provide a very basic glossary to cover ultra-cold atoms and more advanced technologies, which have largely been used only in laboratories.

Bose-Einstein condensate

State of matter formed when an ensemble of atoms at low density is cooled to temperatures very close to absolute zero. In these conditions, most atoms occupy the lowest quantum state, and the whole system is described by a single wavefunction. This allows observing at a macroscopic scale quantum phenomena, such as wavefunction interference, which are typical of the microscopic quantum world. It is common to employ the "cold" label to indicate atoms at temperature low enough (i.e. ~μ°K) to allow interference in the wavefunction of each single atom: in this case, the overall signal generated by the atomic cloud is given by the incoherent contributions of each atom, so that it will scale with the square root of the number of atoms. Conversely, the label "ultra-cold" is used for atoms at temperatures so low (i.e. ~n°K) that a Bose-Einstein condensate is formed, so that interference takes place in the overall wavefunction describing the entire condensate: the contribution of each atom contributes coherently to the total signal, which will therefore scale linearly with the number of atoms.

Molasses cooling, optical molasses, magneto-optical trap

With molasses cooling is indicated a technique used to cool atoms by using laser beams and exploiting Doppler effect. In one dimension, an optical molasses consists of two counter-propagating beams, with frequency tuned slightly below an atomic absorption resonance. The motion of an atom along the direction of the beams will lead to a Doppler shift, so that the absorption rate of the photons travelling in the direction opposed to the atomic motion is increased, whereas the absorption rate of the photons travelling in the other direction is reduced. The momentum exchanged between atoms and laser photons therefore creates a force which is always directed against the motion. A three-dimensional optical molasses can be made with six laser beams, propagating e.g. in three orthogonal directions, and will reduce the velocity in any direction of space, thus reducing the temperature of an atomic cloud, typically to the ~μ°K range. It is to be noted that optical cooling does not confine atoms, so that a magnetic field is typically employed to prevent the dispersion of the atomic cloud. The combination of magnetic confinement with a laser cooling mechanism is commonly known as magneto-optic trap (MOT).

Evaporative cooling, delta-kick cooling, delta-kick collimation

The further cooling needed to obtain ultra-cold atoms from cold ones can be accomplished by several different techniques. In evaporative cooling the overall temperature of the cloud is reduced by removing the hottest atoms: this is accomplished by decreasing the trap depth, so that the atoms with the highest kinetic energy leave it. The technique is analogous to cooling a hot cup of coffee by blowing on it, and the price to be paid is a reduction in the number of atoms.

In delta-kick cooling the harmonic potential of the confining trap is repeatedly switched on and off. During the switched-off intervals the atomic cloud expands, and atoms with differing momentum separate in space. A hotter atom, i.e. one with higher momentum, will travel further afield, and when the confining potential is switched-on back again it will receive a stronger kick directed towards the center of the trap. If the pulse width is set to

an appropriate value determined by the free expansion rate, the atomic momentum will be changed by an amount proportional to the distance the atom has traveled, and all the atoms will be nearly at rest after the kick. In practice, several factors prevent this ideal behaviour and the procedure must be repeated: the process is therefore slow, but the advantage is the number of atoms remains approximately constant. Variations on the delta-kick technique theme allow controlling the expansion dynamics of an atomic cloud, keeping it collimated.

Optical Bloch lattices

Optical lattices are created by the interference of counter-propagating laser beams: the resulting standing wave induces an AC-Stark shift in atoms and acts as a periodic atomic trap. Optical lattices are very versatile tools, easily tuned via the laser setup, and allow unprecedented control over the quantum state of the atoms: as a consequence, they gave rise to a thriving line of research. Atoms loaded from a BEC are densely packed in an optical lattice, and in practice all of them occupy the lowest Bloch band – hence the moniker. By rapidly switching on and off an optical lattice, the atomic wavefunction can be split, and a condensate can thus be divided in two. If the frequencies of the counter-propagating laser beams are slightly detuned a travelling wave is generated instead of the standing one, and an optical Bloch lattice can be employed to transport a Bose-Einstein condensate, e.g. from the atomic cooling stages into an interferometer, and then along it.

Large momentum transfer atom optics, high recoil laser pulse, double Raman transition

Several techniques are being developed to enhance the sensitivity of a CAI interferometer by increasing the separation of the atomic wavepackets, which can be accomplished by implementing large momentum transfer at the atomic beam splitters: if N photon momenta are transferred, an N-fold increase in sensitivity follows[28]. A quick list of possibilities to implement such high-recoil laser pulses includes double Raman transitions, double Bragg diffraction, high-order Bragg diffraction, sequences of Bragg pulses, Bloch oscillations in accelerated optical lattices, combination of Bloch oscillation and high-order Bragg pulses, and frequency-swept rapid adiabatic passage[29]. Different levels of performances have been reached, using techniques at different maturity levels.

A double Raman transition make use of two pairs of counter-propagating pulses for each of the three transitions necessary to have a $\pi/2$-π-$\pi/2$ interferometer[30]: at each beam splitter an atom interacts with four laser beams, which drive two simultaneous Raman transitions and achieve a symmetric momentum-space splitting of $4\hbar k$ instead of $2\hbar k$, thus doubling the interferometer area and thus its sensitivity. By using multi-pulse sequence techniques the scheme can be extended to perform a $4N\hbar k$ momentum splitting.

[28] "Taking atom interferometric quantum sensors from the laboratory to real-world applications", Kai Bongs et al, Nat. Rev. Phys. Vol.1, 731–739 (2019)
https://www.nature.com/articles/s42254-019-0117-4?proof=true&draft=collection%3Fproof%3Dtrue

[29] "High-accuracy inertial measurements with cold-atom sensors", R. Geiger et al., AVS Quantum Sci. 2, 024702 (2020), https://avs.scitation.org/doi/10.1116/5.0009093

[30] "Enhancing the Area of a Raman Atom Interferometer Using a Versatile Double-Diffraction Technique", T. Lévèque, A. Gauguet, F. Michaud, F. Pereira Dos Santos, and A. Landragin, Phys. Rev. Lett. 103, 080405, 2009
https://journals.aps.org/prl/abstract/10.1103/PhysRevLett.103.080405

7 Conclusions

An analysis of the published peer-reviewed scientific literature evidences a widespread consensus that satellite-based gravity missions to be deployed within the next ~10 years will make use of enhanced versions of already deployed technologies. In the meanwhile, cold atom interferometry will start to be employed in space for dedicated scientific missions aimed at testing fundamental assumptions of theoretical physics: in this regard, several proposals have been elaborated, which are now at different implementation stages. Conversely, the use of cold atom interferometry for an Earth Observation gravity mission aimed at geophysics and geodesy scientific objectives with concrete applications is to be considered a long-term challenge, and the scientific community working on space-bound CAI-based gravity sensing has agreed on the following points:

- Ultra-cold atoms in Bose-Einstein condensates (BEC) must be used, and all the most advanced techniques for controlling and detecting the atomic wavefunction (e.g. sub-n°K temperatures, delta-kick cooling, optical lattices, interleaving, point-source interferometry) will be required, which have never been employed simultaneously in laboratory experiments. Therefore, any available assessment on the performance of a CAI-based solution for satellite-based gravity sensing is founded on theoretical assumptions and numerical simulations.
- The deployment of CAI gravity sensors for EO will require the support of conventional technologies to build subsystems and devices (e.g. tilting mirrors, gyroscopes, attitude and orbit control systems) with functional specification which are, to different degrees, beyond the present state of the art. In other terms, several "classical" technologies must improve and enhance their performances beyond what is presently doable to allow the exploitation of the expected performances of a CAI-based solution.
- The actual advantages of CAI-based sensors in terms of gravity field recovery (e.g. the geoid error height at the various spherical degrees, the spatial and temporal resolution, etc.) have not yet been clearly assessed by detailed mission simulation scenarios. Further work and interdisciplinary collaborations are needed, involving not only technology experts but also the scientific communities who make actual use of satellite data to develop models of geophysics and geodesy phenomena.
- Hybrid accelerometers, in which CAI is leveraged to provide a flat noise spectrum and a high bias stability to conventional accelerometers, are presently being developed and could possibly be employed in a shorter timescale. However, available simulations show that they will have an appreciable impact on the gravity field recovery performance only if they can reach a quasi-ideal behaviour. Although in principle possible in a microgravity environment, the actual achievability of the required performances level is very hard to demonstrate via experiments conducted in the presence of gravity.

In the international scene, the USA is playing an important role in the use of CAI for scientific missions aimed at fundamental physics, and has deployed and successfully operated a dedicated Cold Atom Laboratory in the ISS where a BEC has recently been generated (see e.g. https://coldatomlab.jpl.nasa.gov/). However, only low-key preparatory activities seem to be pursued in view of the possible use of CAI for a gravity EO mission: for example, gravity gradiometers prototypes are being developed by NASA-funded projects at CalTech and at Stanford, via the start-up AOSense[31], although some of these groups seem not to have been active for more than 10 years. A detailed vision

[31] https://quantum.jpl.nasa.gov/?page_id=133 (2007);
"Towards a space-borne quantum gravity gradiometer: progress in laboratory demonstration" Nan Yu, James M. Kohel, James R. Kellogg, and Lute Maleki, Jet Propulsion Laboratory and California Institute of Technology, https://www.semanticscholar.org/paper/Progress-towards-a-space-borne-quantum-gravity-Yu-Kohel/761c9b17e55a08ac747159f32e6329282ddb68f0; (2004)
NASA-Goddard & AOSense: CAI gravity gradiometer https://www.nasa.gov/feature/goddard/2018/nasa-industry-team-creates-and-demonstrates-first-quantum-sensor-for-satellite-gravimetry (2018)

for the future was expected at the "2020 NASA Fundamental Physics and Quantum Technology Workshop" (see https://www.aps.org/units/damop/nasa-workshop.cfm) which should have taken place on April 5-7, 2020 in Ventura (CA), but the event has been postponed due to the Coronavirus emergency.

With regards to China, despite all the support the government is giving to quantum technologies (including satellite-based quantum communications) and the publicity usually given to its quantum projects, we have not been able to find any information on activities or plans for a satellite-based CAI gravimetry mission. However, it must be acknowledged that several Chinese research institutions have in the last years reached the capability to obtain ultra-cold atoms at p°K temperatures, and an atomic cooling experiment seems to be planned for the Chinese Space Station (expected to launch in 2022), with a target temperature of below 100 p°K[32,33]. In addition, an analysis of patent applications on cold atom interferometry indicated that China has acquired significant capabilities in the field, especially about the related enabling technologies[34].

We emphasise that the above statements on China and the USA are based solely on an analysis of the available published scientific literature. A complete picture about their plans for possible gravimetry missions exploiting cold atom interferometry would require access to policy sources and preparatory scientific debates, which – if existent - are likely to be outside the public domain.

The ESA has several running programmes which foresee the use of CAI in the framework of scientific missions: coherently, it is pursuing a detailed technology development roadmap, which includes support for enabling technologies, development of accelerometers and gravity gradiometers, and mission simulations. ESA is also analysing the feasibility of a CAI accelerometer for an atmospheric drag mission based on a CubeSat, with the objective of studying thermospheric density and winds. In addition to technology testing, the scientific results of this mission will have important implications for any future gravity mission, which will unavoidably rely on low-flying satellites. Additionally, ESA has highlighted the opportunity of establishing a dedicated microgravity laboratory, where CAI techniques to be used in space could be tested in gravity conditions similar to the ones in which they will actually be employed.

As we have seen, several European national space agencies are funding research projects which involve the use of CAI in space. The French CNES is proposing to make use of CAI in its "Programme Physique Fondamentale et Mesures de Précision", while the German DLR and the Italian ASI are funding research activities on space-based CAI gravity sensing. Indeed, a wide scientific community agrees that a CAI technology demonstration science mission to be deployed in the next ~5 years would be an important milestone, whose results will have important implications for the definition of a full-fledged CAI gravity mission. The EU could consider providing support to such endeavour, which will contribute to pave the way for a CAI gravimetry Earth Observation mission.

[32] "The Emergence of Pico-Kelvin Physics", Xuzong Chen and Bo Fan, Reports on Progress in Physics, Volume 83, Number 7, 2020, https://arxiv.org/ftp/arxiv/papers/2005/2005.01304.pdf

[33] "Comparison of different techniques in optical trap for generating picokelvin 3D atom cloud in microgravity", Hepeng Yao, Tian Luan, Chen Li, Yin Zhang, Zhaoyuan Ma, Xuzong Chen, Optics Communications, Volume 359, Pages 123-128, 2016, https://www.sciencedirect.com/science/article/abs/pii/S0030401815301449?via%3Dihub

[34] "Patent analysis of selected quantum technologies", M. Travagnin, 2019, JRC115251
https://ec.europa.eu/jrc/en/publication/patent-analysis-selected-quantum-technologies

References

[1] "Cold atom interferometry sensors: physics and technologies. A scientific background for EU policymaking", M. Travagnin, JRC121223, 2020; https://ec.europa.eu/jrc/en/publication/cold-atom-interferometry-sensors-physics-and-technologies

[2] "Cold atom interferometry for inertial navigation sensors. Technology assessment: space and defence applications", M. Travagnin, JRC121225, 2020; (Sensitive, limited distribution)

[3] "The ESA Earth Observation Programmes Activities for the Preparation of the Next Generation Gravity Mission", L. Massotti et at., Guidance, Navigation, and Control Conference, 2013 https://www.researchgate.net/publication/268469839_The_ESA_Earth_Observation_Programmes_Activities_for_the_Preparation_of_the_Next_Generation_Gravity_Mission

[4] "Lectures on gravity field basics and GRACE", R. Forsberg, ESA Cryosphere Training Course, 2016 http://seom.esa.int/cryotraining2016/files/CTC16/Day4/3_Forsberg_grace_sep2016%202.pdf

[5] "Progress in satellite gravity recovery from implemented CHAMP, GRACE and GOCE and future GRACE-FO missions", Zheng Wei et al., Geodesy and Geodynamics, Vol. 6, No. 4, 2015 https://www.sciencedirect.com/science/article/pii/S1674984715000506

[6] "Next Generation Gravity Mission", Stefano Cesare and Gianfranco Sechi, Space Technology Library, Vol. 31, 2013; https://link.springer.com/chapter/10.1007/978-1-4614-4541-8_20

[7] "Science and User Needs for Observing Global Mass Transport to Understand Global Change and to Benefit Society", R. Pail et al., Surv. Geophys. 36, 2015; https://link.springer.com/article/10.1007/s10712-015-9348-9

[8] "ESA's next-generation gravity mission concepts", R. Haagmans et al., Rendiconti Lincei. Scienze Fisiche e Naturali, Rend. Fis. Acc. Lincei, 2020 ; https://link.springer.com/article/10.1007/s12210-020-00875-0

[9] "GOCE gradiometer – a guide for users", C. Stummer et al, FGS workshop, 2008; http://www.fs.wettzell.de/veranstaltungen/fgs/workshop2008/poster/FGS2008_Stummer.pdf

[10] "Goce gravity mission", ESA publication office, 2006; http://www.esa.int/esapub/br/br209/br209.pdf

[11] "GOCE gravitational gradiometry", Reiner Rummel, Weiyong Yi, and Claudia Stummer, Journal of Geodesy Vol. 85, No. 777, 2011; https://link.springer.com/article/10.1007/s00190-011-0500-0

[12] "The GRACE Gravity Sensor System", Björn Frommknecht et al., System Earth via Geodetic-Geophysical Space Techniques, 105-118, 2010; https://link.springer.com/chapter/10.1007/978-3-642-10228-8_9

[13] "Gravitation and Geodesy with Inertial Sensors, from Ground to Space", P. Touboul et al., Journal of aerospace Lab, Issue 12, 2016; http://www.aerospacelab-journal.org/sites/www.aerospacelab-journal.org/files/AL12-11.pdf

[14] "A new generation of ultra-sensitive electrostatic accelerometers for GRACE Follow-on and towards the next generation gravity missions", B. Christophe et al., Acta Astronautica 117, 1-7, 2015; https://www.sciencedirect.com/science/article/abs/pii/S0094576515002660

[15] "The measurement of surface gravity", David Crossley et al., Reports on Progress in Physics, Vol. 76, No. 046101, 2013; https://iopscience.iop.org/article/10.1088/0034-4885/76/4/046101

[16] "Status of Development of the Future Accelerometers for Next Generation Gravity Missions", B. Christophe et al., International Symposium on Advancing Geodesy in a Changing World, pp. 85-89, 2018; https://link.springer.com/chapter/10.1007/1345_2018_42

[17] "Cold Atom Interferometers for Future Inertial Sensors and Gradiometers", O. Carraz, Alpbach Summer School presentation, 2019; https://www.summerschoolalpbach.at/docs/2019/lectures/Carraz_QT_ESA.pdf

[18] "Impact of a novel hybrid accelerometer on satellite gravimetry performance", P. Abrykosov et al., Advances in Space Research 63, 3235–3248, 2019; https://hal.archives-ouvertes.fr/hal-02315304/document

[19] "The gravity field and the Global Geodetic Observing System (GGOS)", Journal of Geodynamics Vol. 40, No. 4-5, 387-393, 2005; https://www.sciencedirect.com/science/article/abs/pii/S0264370705000700?via%3Dihub

[20] "Correlated atom accelerometers for mapping the Earth gravity field from Space", T. Lévèque et al., Proceedings Volume 11180, International Conference on Space Optics — ICSO 2018, 111800W, 2019; https://www.spiedigitallibrary.org/conference-proceedings-of-spie/11180/111800W/Correlated-atom-accelerometers-for-mapping-the-Earth-gravity-field-from/10.1117/12.2535951.full?SSO=1

[21] "Observation of Bose–Einstein condensates in an Earth-orbiting research lab", David C. Aveline et al., Nature, Vol. 582, pages 193–197, 2020; https://www.nature.com/articles/s41586-020-2346-1 https://www.researchgate.net/publication/342102533_Observation_of_Bose-Einstein_condensates_in_an_Earth-orbiting_research_lab

[22] "Space-borne Bose-Einstein condensation for precision interferometry", D. Becker et al., Nature volume 562, pages 391–395, 2018; https://www.nature.com/articles/s41586-018-0605-1 https://arxiv.org/pdf/1806.06679.pdf

[23] "The Future of the Satellite Gravimetry after the GOCE Mission", P. Silvestrin et al., International Association of Geodesy Symposia, Vol. 136, 223-230, 2012; https://link.springer.com/chapter/10.1007%2F978-3-642-20338-1_27

[24] "A spaceborne gravity gradiometer concept based on cold atom interferometers for measuring Earth's gravity field", O. Carraz et al, Microgravity Science and Technology, Vol. 26, 2014; https://link.springer.com/article/10.1007/s12217-014-9385-x

[25] "Simulation-based evaluation of a cold atom interferometry gradiometer concept for gravity field recovery", K. Douch et al., Advances in Space Research 61 1307–1323, 2018 https://hal.sorbonne-universite.fr/hal-01826234/document

[26] "Concept study and preliminary design of a cold atom interferometer for space gravity gradiometry", A. Trimeche et al., Class. Quantum Grav. **36,** 215004, 2019 https://iopscience.iop.org/article/10.1088/1361-6382/ab4548

[27] "MOCASS: A Satellite Mission Concept Using Cold Atom Interferometry for Measuring the Earth Gravity Field", F. Migliaccio et al., Surveys in Geophysics, 40, 2019 https://link.springer.com/article/10.1007/s10712-019-09566-4

[28] "Taking atom interferometric quantum sensors from the laboratory to real-world applications", Kai Bongs et al, Nat. Rev. Phys. Vol.1, 731–739, 2019 https://www.nature.com/articles/s42254-019-0117-4?proof=true&draft=collection%3Fproof%3Dtrue

[29] "High-accuracy inertial measurements with cold-atom sensors", R. Geiger et al., AVS Quantum Sci. 2, 024702 (2020), https://avs.scitation.org/doi/10.1116/5.0009093

[30] "Enhancing the Area of a Raman Atom Interferometer Using a Versatile Double-Diffraction Technique", T. Lévèque, A. Gauguet, F. Michaud, F. Pereira Dos Santos, and A. Landragin, Phys. Rev. Lett. 103, 080405, 2009 https://journals.aps.org/prl/abstract/10.1103/PhysRevLett.103.080405

[31] https://quantum.jpl.nasa.gov/?page_id=133, 2007;
Jet Propulsion Laboratory and California Institute of Technology: "Towards a space-borne quantum gravity gradiometer: progress in laboratory demonstration", Nan Yu et al., 2004 https://www.semanticscholar.org/paper/Progress-towards-a-space-borne-quantum-gravity-Yu-Kohel/761c9b17e55a08ac747159f32e6329282ddb68f0;
NASA-Goddard & AOSense: CAI gravity gradiometer https://www.nasa.gov/feature/goddard/2018/nasa-industry-team-creates-and-demonstrates-first-quantum-sensor-for-satellite-gravimetry, 2018

[32] "The Emergence of Pico-Kelvin Physics", Xuzong Chen and Bo Fan, Reports on Progress in Physics, Volume 83, Number 7, 2020, https://arxiv.org/ftp/arxiv/papers/2005/2005.01304.pdf

[33] "Comparison of different techniques in optical trap for generating picokelvin 3D atom cloud in microgravity", Hepeng Yao, Tian Luan, Chen Li, Yin Zhang, Zhaoyuan Ma, Xuzong Chen, Optics Communications, Volume 359, Pages 123-128, 2016 https://www.sciencedirect.com/science/article/abs/pii/S0030401815301449?via%3Dihub

[34] "Patent analysis of selected quantum technologies", M. Travagnin, JRC115251, 2019 https://ec.europa.eu/jrc/en/publication/patent-analysis-selected-quantum-technologies

List of abbreviations and definitions

A-O noise:	Atmospheric-Oceanic noise
ADS:	Amplitude Spectral Density
AOCS:	Attitude and Orbit Control System
ASI:	Agenzia Spaziale Italiana
BEC:	Bose-Einstein Condensate (or Condensation)
CAI:	Cold Atom Interferometry
CGE:	Cumulative Geoid Error
CHAMP:	Challenging Minisatellite Payload
CNES:	Centre national d'études spatiales
DKC:	Delta Kick Cooling
DLR:	Deutschen Zentrum für Luft und Raumfahrt (German Aerospace Center)
EO:	Earth Observation
ESTEC:	European Space Research and Technology Centre (of ESA)
GIA:	Glacial Isostatic Adjustment
GGT:	Gravity Gradient Tensor
GOCE:	Gravity field and steady-state Ocean Circulation Explorer
GRACE:	Gravity Recovery And Climate Experiment
GRACE-FO:	GRACE follow-on
GRICE:	Gradiométrie à Interféromètres quantiques Corrélés pour l'Espace
IMB:	Ice Mass Balance
IUGG:	International Union of Geodesy and Geophysics
LL-SST:	Low-Low Satellite-Satellite Tracking
LNE:	Laboratoire National de Métrologie et d'Essais
MOCASS:	Mass Observation with Cold Atom Sensors in Space
MOT:	Magneto-Optical Trap
NGGM:	Next Generation Gravity Mission
ONERA:	Office National d'Etudes et de Recherches Aérospatiales
PSI:	Point Source interferometry
PSD:	Power Spectral Density
SGG	Satellite gravity gradiometry
SH:	Spherical Harmonic
SL:	Sea Level
SST	Satellite-to-satellite tracking
SWaP:	Size, Weight and Power
SYRTE:	Systèmes de Référence Temps-Espace
ZARM:	Zentrum für Angewandte Raumfahrttechnologie und Mikrogravitation (Center of Applied Space Technology and Microgravity)

GETTING IN TOUCH WITH THE EU

In person

All over the European Union there are hundreds of Europe Direct information centres. You can find the address of the centre nearest you at: https://europa.eu/european-union/contact_en

On the phone or by email

Europe Direct is a service that answers your questions about the European Union. You can contact this service:

- by freephone: 00 800 6 7 8 9 10 11 (certain operators may charge for these calls),

- at the following standard number: +32 22999696, or

- by electronic mail via: https://europa.eu/european-union/contact_en

FINDING INFORMATION ABOUT THE EU

Online

Information about the European Union in all the official languages of the EU is available on the Europa website at: https://europa.eu/european-union/index_en

EU publications
You can download or order free and priced EU publications from EU Bookshop at: https://publications.europa.eu/en/publications. Multiple copies of free publications may be obtained by contacting Europe Direct or your local information centre (see https://europa.eu/european-union/contact_en).

KJ-NA-30371-EN-N

The European Commission's science and knowledge service

Joint Research Centre

JRC Mission

As the science and knowledge service of the European Commission, the Joint Research Centre's mission is to support EU policies with independent evidence throughout the whole policy cycle.

EU Science Hub

ec.europa.eu/jrc

@EU_ScienceHub

EU Science Hub - Joint Research Centre

Joint Research Centre

EU Science Hub

Publications Office of the European Union

doi:10.2760/225071

ISBN 978-92-76-21686-5